Arch Toxicol
DOI 10.1007/s00204-017-1967-0

MOLECULAR TOXICOLOGY

Chalcone flavokawain B induces autophagic-cell death via reactive oxygen species-mediated signaling pathways in human gastric carcinoma and suppresses tumor growth in nude mice

Chia-Ting Chang[1] · You-Cheng Hseu[2,3] · Varadharajan Thiyagarajan[2] · Kai-Yuan Lin[4] · Tzong-Der Way[5] · Mallikarjuna Korivi[1] · Jiuun-Wang Liao[6] · Hsin-Ling Yang[1]

Received: 9 December 2016 / Accepted: 21 March 2017

Abstract Flavokawain B (FKB), a naturally occurring chalcone in kava extracts, has been reported to possess anticancer activity. However, the effect of FKB on gastric cancer remains unclear. We examined the in vitro and in vivo anticancer activity and autophagy involvement of FKB and determined the underlying molecular mechanisms. FKB is potently cytotoxic to human gastric cancer cells (AGS/NCI-N87/KATO-III/TSGH9201) and mildly toxic towards normal (Hs738) cells and primary mouse hepatocytes. FKB-induced AGS cell death was characterized by autophagy, not apoptosis, as evidenced by increased LC3-II accumulation, GFP-LC3 puncta and acidic vesicular organelles (AVOs) formation, without resulting procaspase-3/PARP cleavage. FKB further caused p62/SQSTM1 activation, mTOR downregulation, ATG4B inhibition, and Beclin-1/Bcl-2 dysregulation. Silencing autophagy inhibitors CQ/3-MA and LC3 (shRNA) significantly reversed the FKB-induced cell death of AGS cells. FKB-triggered ROS generation and ROS inhibition by NAC pre-treatment diminished FKB-induced cell death, LC3 conversion, AVO formation, p62/SQSTM1 activation, ATG4B inhibition and Beclin-1/Bcl-2 dysregulation, which indicated ROS-mediated autophagy in AGS cells. Furthermore, FKB induces G_2/M arrest and alters cell-cycle proteins through ROS-JNK signaling. Interestingly, FKB-induced autophagy is associated with the suppression of HER-2 and PI_3K/AKT/mTOR signaling cascades. FKB inhibits apoptotic Bax expression, and Bax-transfected AGS cells exhibit both apoptosis and autophagy; thus, FKB-inactivated Bax results in apoptosis inhibition. In vivo data demonstrated that FKB effectively inhibited tumor growth, prolonged the survival rate, and induced autophagy in AGS-xenografted mice. Notably, silencing of LC3 attenuated FKB-induced autophagy in AGS-xenografted tumors. FKB may be a potential chemopreventive agent in the activation of ROS-mediated autophagy of gastric cancer cells.

Keywords Flavokawain B · AGS cells · Autophagy · ROS · ATG4B

Abbreviations

FKB	Flavokawain B
MTT	3-(4,5-dimethylthiazol-2-yl)-2,5-diphenyltetrazolium bromide
LC3	Microtubule-associated light chain 3
AVO	Acidic vesicular organelle
PARP	Poly (ADP-ribose) polymerase
CQ	Chloroquine

Chia-Ting Chang and You-Cheng Hseu contributed equally.

✉ You-Cheng Hseu
ychseu@mail.cmu.edu.tw

✉ Hsin-Ling Yang
hlyang@mail.cmu.edu.tw

1 Institute of Nutrition, College of Biopharmaceutical and Food Sciences, China Medical University, 91, Hsueh-Shih Road, Taichung 40402, Taiwan

2 Department of Cosmeceutics, College of Biopharmaceutical and Food Sciences, China Medical University, 91, Hsueh-Shih Road, Taichung 40402, Taiwan

3 Department of Health and Nutrition Biotechnology, Asia University, Taichung 41354, Taiwan

4 Department of Medical Research, Chi-Mei Medical Center, Tainan 710, Taiwan

5 Department of Life Sciences, College of Biopharmaceutical and Food Sciences, China Medical University, Taichung 40402, Taiwan

6 Graduate Institute of Veterinary Pathology, National Chung-Hsing University, Taichung 402, Taiwan

Published online: 03 April 2017

3-MA	3-Methyladenine
ROS	Reactive oxygen species
$DCFH_2$-DA	2′,7′-dihydrofluorescein-diacetate
NAC	*N*-acetyl-L-cysteine
p38 MAPK	p38 mitogen-activated protein kinase
JNK	c-jun N-terminal kinase
ERK	Extracellular signal-regulated protein kinase
CDC25C	Cell division cycle 25 °C
PI3K	Phosphatidylinositol 3-kinase
HER2	Human epidermal growth factor receptor 2

Introduction

Gastric cancer is one of the most common malignant cancers, and it is the second leading cause of death from cancer worldwide. According to the Cancer Registry Annual Report of Taiwan, gastric cancer is the eighth cause of all cancer incidences and the fifth cause of all cancer deaths in Taiwan (Huang et al. 2007). Gastric cancer is often diagnosed at an advanced stage, because there are no early signs or symptoms. To date, chemotherapy is the treatment of choice for gastric cancer; however, the curative effects of chemotherapeutic drugs often lead to substantial side effects, which include hepatotoxicity, immunosuppression, and myelosuppression (Zhang et al. 2014). Thus, the development of effective chemopreventive or chemotherapeutic agents using non-toxic botanicals may represent one strategy for the management of gastric cancers.

Autophagy is a catabolic process that plays a pivotal role in the homeostatic process of degradation and recycling defective organelles and aggregated or long lived proteins. This process may be stimulated in response to different stress situations, such as starvation, irradiation, oxidative stress, hypoxia, and chemical insults (Ohsumi 2001). Autophagy involves the formation of double-membrane vesicles, referred to as autophagosomes, which engulf intracellular contents, such as endoplasmic reticulum, mitochondria, and ribosomes, and fuse with lysosomes for degradation (Xie et al. 2011). Autophagy has been associated not only with tumor cell survival mechanisms but also with tumor suppression mechanisms via the removal of damaged organelles and proteins. Several molecular and cell signaling pathways have been implicated in the regulation of autophagy, such as microtubule-associated light chain 3 (LC3), mammalian target of rapamycin (mTOR), and Beclin-1 (Kang et al. 2011). Several chemotherapeutic drugs and many natural compounds have been demonstrated to trigger caspase-independent autophagic-cell death via activation of the autophagy signaling pathway (Kondo et al. 2005). Recent studies suggested that ROS induce autophagic-cell death, which provides a novel strategy for cancer treatment (Zhou et al. 2014). The role of autophagy during cancer therapy is complex; however, autophagy is becoming an attractive approach for anticancer therapies.

Plant-derived natural products have received extensive attention in cancer therapy because of their promising efficacy, low toxicity towards normal tissues and reduction in chemotherapy-associated side effects (Zhang et al. 2012). The kava–kava plant (*Piper methysticum*) is a perennial shrub native to the ethnogeographic regions of Polynesia, Melanesia, and Micronesia. An epidemiologic study demonstrated that the consumption of kava root extracts was associated with a decreased incidence of cancer in the Pacific Islands (Steiner 2000). Chalcones are a precursor of flavonoids, mainly extracted from the roots of kava–kava plant, and have been demonstrated to exhibit promising anticancer, anti-inflammatory, and antinociceptive properties (Abu et al. 2013). Studies suggest that the kava chalcone (50 mg/kg of body weight) effectively suppressed the in vivo growth rate of bladder cancer xenograft cells (RT4 cells), without causing toxicity, in athymic nude mice (Zi and Simoneau 2005). Among the chalcones, flavokawain B (FKB) exhibits a growth inhibitory effect in various cancers, such as breast cancer, osteosarcoma, bladder cancer, and synovial sarcoma, through several signaling pathways (Abu et al. 2015).

Recent concerns have arisen regarding the safety of kava and its associated liver injury. To date, there is limited evidence that the primary psychoactive constituents (kavalactones) or other constituents (pipermethystine and FKB) of kava plants exhibit hepatotoxicity. Studies suggest that kava may be hepatotoxic as a result of overdose or comedication and that it is likely triggered by an unacceptable quality of the raw material (Teschke 2010). Chalcone-based flavokawains A (FKA) and FKB in kava recapitulated its hepatotoxic synergism with acetaminophen, whereas dihydromethysticin (DHM, a representative kavalactone and a potential lung cancer chemopreventive agent) had no effect. The organic solvent fraction exhibited a stronger toxicity, whereas the aqueous extract exhibited an apparently safe history (Zhou et al. 2010). For the first time, these results demonstrate the hepatotoxic risk of kava and its chalcone-based FKA and FKB in vivo and suggest that an herb-drug interaction may account for the rare hepatotoxicity associated with (anxiolytic) kava usage in humans (Narayanapillai et al. 2014). Recently, Germany's Federal Administrative Court abrogated the ban of kava consumption in 2014 (Carreñ OI 2014).

Many studies have reported the anticancer effectiveness of FKB; however, the specific mechanism of FKB has not been clearly elucidated. Thus, the present study was designed to investigate the potential therapeutic effects of FKB on human gastric cancer (AGS) cells. This study further aimed to provide in vitro or in vivo evidence that autophagy plays an important role in FKB-induced cell

death, instead of apoptosis, as well as to distinguish the role of ROS signaling that underlies the induction of autophagic pathways.

Materials and methods

Chemicals and antibodies

Roswell Park Memorial Institute (RPMI-1640) medium, Dulbecco's Modified Eagle Medium (DMEM), Iscove modified Dulbecco medium (IMDM), fetal bovine serum (FBS), glutamine, and penicillin/streptomycin were purchased from Invitrogen (Carlsbad, CA, USA). Antibodies against LC3B, p62/SQSTM1, PARP, Bax, p-mTOR, mTOR, ATG4B, ATG7, Beclin-1, p-PI3K, PI3K, p-AKT, AKT, p-JNK1/2, JNK1/2, p-ERK1/2, ERK1/2, p-p38, p38, caspase-3, cyclin A, CDC25C, and p-HER2 (#2243) were obtained from Cell Signaling Technology, Inc. (Danvers, MA, USA). Antibodies against Bcl-2, CDK2, p53, and β-actin were purchased from Santa Cruz Biotechnology, Inc. (Heidelberg, Germany). Antibody against GFP was purchased from Gene Tex, Inc. (Irvine, CA, USA). Antibody against Cyclin D1 was purchased from Invitrogen (Carlsbad, CA, USA). Antibodies against HER2 were purchased from Millipore Corp. (Bedford, MA, USA). Antibodies against Cyclin B1 were purchased from Biosoyrce, Inc. (Dacula, GA, USA). All secondary antibodies were purchased from Santa Cruz Biotechnology (Santa Cruz, CA). Z-Val-Ala-Asp-fluoromethylketone (z-VAD-FMK) was obtained from Calbiochem (San Diego, CA, USA). 3-(4,5-dimethylthiazol-2-yl)-2,5-diphenyltetrazolium bromide (MTT), Doxorubicin, acridine orange (AO), propidium iodide (PI), chloroquine (CQ), 3-Methyladenine (3-MA), *N*-acetylcysteine (NAC), and 2′,7′-dihydrofluorescein-diacetate ($DCFH_2$-DA) were obtained from Sigma-Aldrich (St. Louis, MO, USA). JNK inhibitor SP600125, ERK inhibitor U0126, and p38 inhibitor SB203580 were obtained from Calbiochem (La Jolla, CA, USA). All other chemicals were reagent grade or HPLC grade and were supplied by Merck & Co., Inc. (Darmstadt, Germany) or Sigma-Aldrich (St. Louis, MO, USA).

Cell culture

Human gastric adenocarcinoma (AGS), human gastric carcinoma (NCI-N87), human normal mixed cells (stomach and intestine) (Hs738), and human gastric carcinoma (Kato-III) were obtained from the American-Type Culture Collection (Rockville, MD, USA). The TSGH 9201 human gastric cancer cell line was obtained from the Bioresource Collection and Research Center of Taiwan. These cells were grown in RPMI1640, DMEM, or IMDM supplemented with 10% FBS, 2 mM glutamine, and 1% penicillin–streptomycin–neomycin in a humidified incubator (5% CO_2 in the air at 37 °C). Hepatocyte cells were isolated via a two-step collagenase perfusion method. The isolated hepatocytes were suspended in L-15-based culture medium (SAA-omitted Leibovitz L-15 plus 0.5 mmol/L L -methionine and 0.2 mmol/L L-cysteine) that contained 18 mmol/L HEPES, 5 mg/L transferrin, 5 μg/L sodium selenite, 1 g/L galactose, 1×10^5 U/L penicillin, 100 mg/L streptomycin, and 2.5% FBS. Cells (1×10^6) were planted on 3-cm plastic culture dishes pre-coated with type I rat tail collagen and incubated in a 37 °C humidified incubator in an air atmosphere. Twenty-four hours after isolation, the hepatocytes were incubated with L-15-based medium plus FKB for the indicated time. The L-methionine and L -cysteine supplements were freshly prepared. The medium was changed once daily.

Drug treatment

FKB was purchased from LKT Laboratories, Inc. (St. Paul, MN, USA) as described in our previous publication (Hseu et al. 2012). The obtained FKB purity was greater than 99%, which was confirmed via HPLC analysis. A stock solution of FKB (10 mg/mL or 35.2 mM) was prepared in 100% DMSO and subsequently diluted in medium to ensure that the final concentration of DMSO was 0.1% in the medium.

MTT assay

Cells were seeded in 24-well plates at a density of 8×10^4 cells/well. The cells were treated with different concentrations of FKB and incubated for 24 h. After incubation, the cells were washed with PBS and subsequently incubated with 400 μL of 0.5 mg/mL MTT in medium for 2 h. The culture supernatant was removed and re-suspended with 400 μL of DMSO to dissolve MTT formazan; the absorbance was measured at 570 nm using an ELISA microplate reader (Bio-Tek Instruments, Winooski, VT, USA). The effect of FKB on the cell viability was assessed as the percent of viable cells compared with the vehicle-treated control cells, which were arbitrarily assigned a viability of 100%.

Colony formation assay

AGS cells (5×10^5 cells/60 mm dish) were treated with different concentrations of FKB (0–10 μg/mL) for 24 h. The cells were subsequently trypsinized and re-plated at a density of 3×10^4 cells/35 mm dish in triplicate, followed by incubation with RPMI1640 for 7 days. The cells were subsequently fixed with 10% neutral buffered formalin at room

temperature for 10 min and stained with 20% Giemsa solution (Merck, Darmstadt, Germany). The cells were assayed for their ability to proliferate and form colonies, and the numbers of colonies >1 mm in size were counted using a microscope (40× magnification). The percentage of colony formation was calculated by defining the number of colonies in the absence of FKB as 100%.

Measurement of ROS generation

The intracellular accumulation of ROS was detected via fluorescence microscopy using DCFH2-DA. Cells (8×10^4 cells/24-well) were cultured in RPMI1640 supplemented with 10% FBS; the culture medium was renewed when the cells reached 80% confluence. After FKB treatment, the cell culture media were removed, and the cells were washed with PBS and incubated with 10 μM DCFH2-DA in fresh culture medium at 37 °C for 15 min. The acetate groups on DCFH2-DA were removed using an intracellular esterase, thereby trapping the probe inside the AGS cells. The intracellular ROS, as indicated by DCF fluorescence, were measured with a fluorescence microscope (Olympus 1×71 at 200× magnification). The fluorescence intensity in each condition was quantified from a squared section of fluorescence-stained cells via analysis with LS 5.0 soft-imaging solutions (Olympus Imaging America Inc., Corporate Parkway Centre Valley, PA, USA).

Cell-cycle analysis

The cellular DNA content was determined via flow cytometric analysis with PI-labeled cells. The AGS cells were subsequently blocked with RPMI1640 medium that contained 3 mM thymidine for 16 h. The cell-cycle synchronized cells were then washed with PBS and re-stimulated to enter the G_1 phase together via the addition of fresh RPMI1640 medium that contained FKB (1.25–10 μg/mL). The cells were harvested at 24 h by trypsinization and subsequently fixed in 3 mL of ice cold 70% ethanol at −20 °C overnight. Cell pellets were collected via centrifugation, re-suspended in 500 μL of PI staining buffer (1% Triton X-100, 0.5 mg/mL RNase A, and 4 μg/mL PI in PBS), and incubated at room temperature for 30 min. The cell-cycle progression was detected on a FACScan cytometer (BD Biosciences, San Jose, CA) equipped with a single argon ion laser (488 nm). The cell-cycle profiles were analyzed with the ModFit software (Verity Software House, Topsham, ME).

Western blot analysis

Cells (1×10^6 cells/dish) were seeded in a 10-cm dish and pretreated with FKB. The cells were subsequently washed with cold PBS and re-suspended in lysis buffer that contained 10 mM Tris–HCl [pH 8.0], 0.32 M sucrose, 1% Triton X-100, 5 mM EDTA, 2 mM DTT, and 1 mM phenylmethyl sulfonyl fluoride. The suspension was centrifuged at 12,000×*g* for 20 min at 4 °C. The total protein content was determined with Bio-Rad protein assay reagent (Hercules, CA, USA) using bovine serum albumin as a standard. The proteins were separated via SDS–polyacrylamide gel electrophoresis (SDS–PAGE) and subsequently transferred to PVDF membranes. The blots were blocked with 5% non-fat milk in PBS that contained 1% Tween-20 at room temperature for 1 h and incubated with the appropriate primary antibodies at 4 °C overnight. After a wash, the blots were incubated with peroxidase-conjugated secondary antibody. The blots were imaged using an ImageQuant™ LAS 4000 mini (Fujifilm) system with SuperSignal West Pico chemiluminescence substrate (Thermo Scientific Inc., Rockford, IL, USA).

GFP-LC3 plasmid transfection and GFP-LC3 dot formation

LC3 cDNA was a kind gift from Dr. Tamotsu Yoshimori (Osaka University, Japan) and Dr. Noboru Mizushima (Tokyo Medical and Dental University, Japan). GFP-LC3 fusion protein was used to make the autophagosomes visible in cells. The cells were seeded onto coverslips placed onto a 6-well plate (5×10^5 cells/well). After an overnight culture, the cells were transfected with 2.5 μg of GFP-LC3 that expressed plasmid in each well of a 6-well plate using Lipofectamine 2000 (Invitrogen, Carlsbad, CA, USA) and incubated for 24 h. The medium was removed, and fresh medium that contained FKB was added to the wells. At the end of the FKB treatment, the cells were washed twice with PBS, and the expression of GFP-LC3 dots in AGS was detected using a laser scanning confocal microscope at 200× magnification.

Acridine orange staining

Acridine orange (AO) staining was used to detect the formation of AVOs in AGS cells. After FKB treatment, the cells were washed with PBS twice, followed by staining with AO (1 μg/mL) and dilution in PBS that contained 5% FBS for 15 min. After staining, the cells were washed with PBS and covered with PBS that contained 5% FBS. The cells were observed under a red filter fluorescence microscope, and the formation of AVOs in cells was visualized at 100× magnification and analyzed via flow cytometry. AO is a lysosomotropic metachromatic and weak base membrane-permeant fluorescent dye; its fluorescence emission is concentration dependent from red at

high concentrations (in lysosomes) to green at low concentrations (in the cytosol), with yellow as an intermediate in some conditions.

Transfection of shRNA targeting LC3

The RNAi reagents were obtained from the National RNAi Core Facility located at the Institute of Molecular Biology/Genomic Research Center, Academia Sinica (Taipei, Taiwan). Lentivirus infection of AGS cells was used to stably integrate and express short hairpin RNA (shRNA) that targeted the LC3 mRNA sequences. Individual clones are identified by their unique TRC number: shLuc TRCN0000072246 for the vector control targeted to luciferase and shLC3 TRCN0000243391 (responding sequence: AGC GAG TTG GTC AAG ATC ATC) targeted to LC3. For the lentivirus-shRNA infection of cells, 5×10^{6} AGS cells were sub-cultured onto a 60-mm dish. After 16 h of culture, the cells were infected with recombinant lentivirus vectors at a multiplicity of infection of 1. The next day, the medium was removed, and the cells were selected by 2 μg/mL puromycin for 2 days. The detailed steps for the production of lentivirus have been previously described (Hsin et al. 2010).

Bax transfection

AGS cells were transfected with Bax or vector alone (True ORF Gold, RC204369) using Lipofectamine 2000 according to the manufacturer's instructions. For the transfection, AGS cells (5×10^{6} cells) were grown in RPMI1640 that contained 10% FBS and plated in a 60-mm dish. On the next day, the culture medium was replaced with 500 μL of Opti-MEM, and the cells were transfected using Lipofectamine 2000 transfection reagent. For each transfection, 5 μL of Lipofectamine 2000 were mixed with 250 μL of Opti-MEM and incubated for 5 min at room temperature. In a separate tube, BAX (2 μg in 250 μL of Opti-MEM) was added to 250 μL of Opti-MEM, and the BAX solution was added to the diluted lipofectamine 2000 reagent. The resulting BAX/lipofectamine 2000 mixture (500 μL) was incubated for an additional 20 min at room temperature to enable complex formation. The solution was subsequently added to the cells in the 60-mm dish for a final transfection volume of 2 mL. After incubation for 6 h, the transfection medium was replaced with 2 mL of standard growth medium, and the cells were cultured at 37 °C. The next day, the medium was removed, and the cells were selected by 200 μg/mL G418 (Sigma-Aldrich, St. Louis, MO, USA). After FKB treatment, the cells were subjected to protein expression and TUNEL assay analyses.

Apoptotic DNA fragmentation

Apoptotic cell death was measured using terminal deoxynucleotidyl transferase-meditated dUTP-fluorescein nick end-labeling (TUNEL) with an in situ cell death detection kit (Roche, Mannheim, Germany) according to the manufacturer's instructions. Cells (2×10^{4} cells/well) were seeded onto an 8-well glass Tek chamber (Nunc, Denmark). After FKB treatment, the cells were washed twice with PBS, fixed in 4% paraformaldehyde for 60 min and subsequently permeabilized with 0.1% Triton X-100 for 5 min at room temperature. The cells were then incubated with TUNEL reaction buffer in a 37 °C humidified chamber for 1.5 h in the dark, rinsed twice with PBS, and incubated with DAPI (1 μg/mL) at 37 °C for 5 min; the stained cells were visualized using a fluorescence microscope at 200× magnification.

Animals

Female athymic nude mice (BALB/*c-nu*), 5–7 weeks of age, were purchased from the National Laboratory Animal Center (Taipei, Taiwan); the mice were maintained in caged housing in a specifically designed pathogen-free isolation facility with a 12 h/12 h light/dark cycle. All mice had free access to water and rodent chow (Oriental Yeast Co Ltd., Tokyo, Japan). The animal experiments strictly followed "The Guidelines for the Care and Use of Laboratory Animals" published by the Chinese Society of Animal Science, Taiwan. The animal protocols were approved by the Institutional Animal Care and Use Committee (IACUC) of China Medical University.

Tumor cell inoculation

Twenty-seven mice (5–7 weeks) were randomly divided into nine groups that contained three animals per group. AGS cells (5×10^{6} cells) were mixed in a 200 μL of matrix gel and then subcutaneously injected into the left hind flanks of the nude mice. After cell inoculation for 7 days, the mice were equally divided into three groups, including the control (0.1% DMSO), FKB intraperitoneal injection (1.5 mg/kg, every 2 days), and FKB oral administration (7.5 mg/kg, every 2 days) groups. In the AGS shLC3-xanografted experiment, the mice were equally divided into six groups, including the wild type (wt), wt + FKB intraperitoneal injection (1.5 mg/kg, every 2 days), shLuc control, shLuc + FKB, shLC3 control, and shLC3 + FKB groups. FKB was freshly dissolved in 0.1% DMSO. To monitor drug toxicity, the body weight of each animal was measured every 3 days. The tumor volumes in the mice were compared with caliper measurements of the tumor length, width, and depth and subsequently calculated every 3 days

using the following formula: length × width^2 × 1/2. On the 51st day, all mice were sacrificed, and the tumor tissues were removed and weighed. A veterinary pathologist examined the mouse organs, including the liver, lung, heart, spleen, and kidney.

Histopathological analyses of xenografted tumor

The biopsied tumor tissues were embedded in paraffin, cut into 3-mm-thick sections, placed in plastic cassettes and immersed in 10% neutral buffered formalin for 7 days. The fixed tissues were routinely processed and subsequently embedded in paraffin, sectioned, deparaffinized, and rehydrated using standard techniques. The extent to which the FKB treatment shrunk the tumor cells was evaluated via the assessment of mitotic cell division in the xenografted tumor sections using hematoxylin and eosin stains.

Western blotting of xenografted tumors

The tumor tissues were homogenized in RIPA buffer that contained 1% protease inhibitor cocktail 1, 1% phosphatase inhibitor cocktail 2, and 1% phosphatase inhibitor cocktail 3 (Sigma-Aldrich, St. Louis, MO, USA); the samples (50 μg of protein) were subjected to electrophoresis on SDS gels (8–15%) and transferred to a PVDF membrane. The remaining steps were followed as previously described in this article.

Animal survival study

Animals were inoculated with AGS cells at day 0, randomized and exposed to treatment from day 1 until death. Sixteen mice were equally divided into two groups, including the control (0.1% DMSO) and FKB (1.5 mg/kg, intraperitoneal injection for every 2 days) groups. The mice were allowed to live until a natural death or were sacrificed with an overdose of pentobarbital in severe clinical conditions to avoid undue suffering. The survival index was evaluated as the ratio between the cumulative survival times of the treated animals and the sham-treated animals. This index was evaluated by summing, for each experimental group, the survival times of the treated mice and dividing this value by the sum of the survival times of the sham-treated mice multiplied by 100.

Statistical analysis

The obtained data were analyzed using analysis of variance (ANOVA), followed by Dunnett's test for pairwise comparison. The mean values are presented with their standard deviations (mean ± SD). Statistical significance was defined as $*p<0.05$, $**p<0.01$, $***p<0.001$ compared with the untreated control cells.

Results

FKB inhibits viability and colony formation ability of human gastric carcinoma cells through induction of autophagy

Human gastric cancer cell lines (AGS, NCI-N87, KATO-III and TSGH9201), a human normal cell line (Hs738) and mouse primary hepatocytes were treated with various concentrations of FKB (0–20 μg/mL) for 24 h. The results from the MTT assay demonstrated that FKB treatment significantly ($p<0.05$) decreased the survival of AGS, NCI-N87, KATO-III, and TSGH 9201 cells in a dose-dependent manner with IC_{50} values of 4.6, 9.5, 9.0, and 12.4 μg/mL, respectively. These results indicate the susceptibility of cancer cells to FKB-induced cell death (Fig. 1a). FKB is cytotoxic to all gastric cancer cells; however, the cytotoxicity of FKB towards AGS cells was more prominent compared with the other cells. Regardless of this difference, FKB toxicity towards normal gastric (Hs738) cells was very minimal with an increased IC_{50} value (17.8 μg/mL, Fig. 1a). We subsequently determined the cytotoxicity of FKB on mouse primary hepatocytes and identified minimal toxicity towards primary mouse hepatocytes (Fig. 1a). The colony formation ability (a characteristic of tumor cells that is closely correlated with tumorigenesis in vivo) was assessed to determine the long-term impact of FKB on cell growth. The colony-forming ability of AGS cells was significantly and dose-dependently suppressed by FKB treatment (Fig. 1b). The reductions in colony number were accompanied by a reduction in the colony size in the AGS cells (Fig. 1b).

As a result of its promising effects on the induction of cancer cell death, we assume that FKB may activate the key regulatory proteins involved in autophagy and/or apoptosis. To determine whether FKB induces autophagy in AGS cells, we initially examined the intracellular distribution of LC3, a promising autophagy marker. Western blot data demonstrated that FKB treatment increased lipidated LC3 form (LC3-II) accumulation in a dose- (0–10 μg/mL) and time-dependent (0–48 h) manner (Fig. 1c, e). This finding is absolute evidence for the initiation of autophagy by FKB in AGS cells. p62, which is also referred to as sequestosome 1 (SQSTM1), is commonly used as a marker to investigate autophagic flux, because it directly binds to LC3 via a specific sequence motif and subsequently degrades itself during autophagy. Interestingly, the expression of p62 protein increased to the maximum level at 24 h (Fig. 1d, e) and subsequently

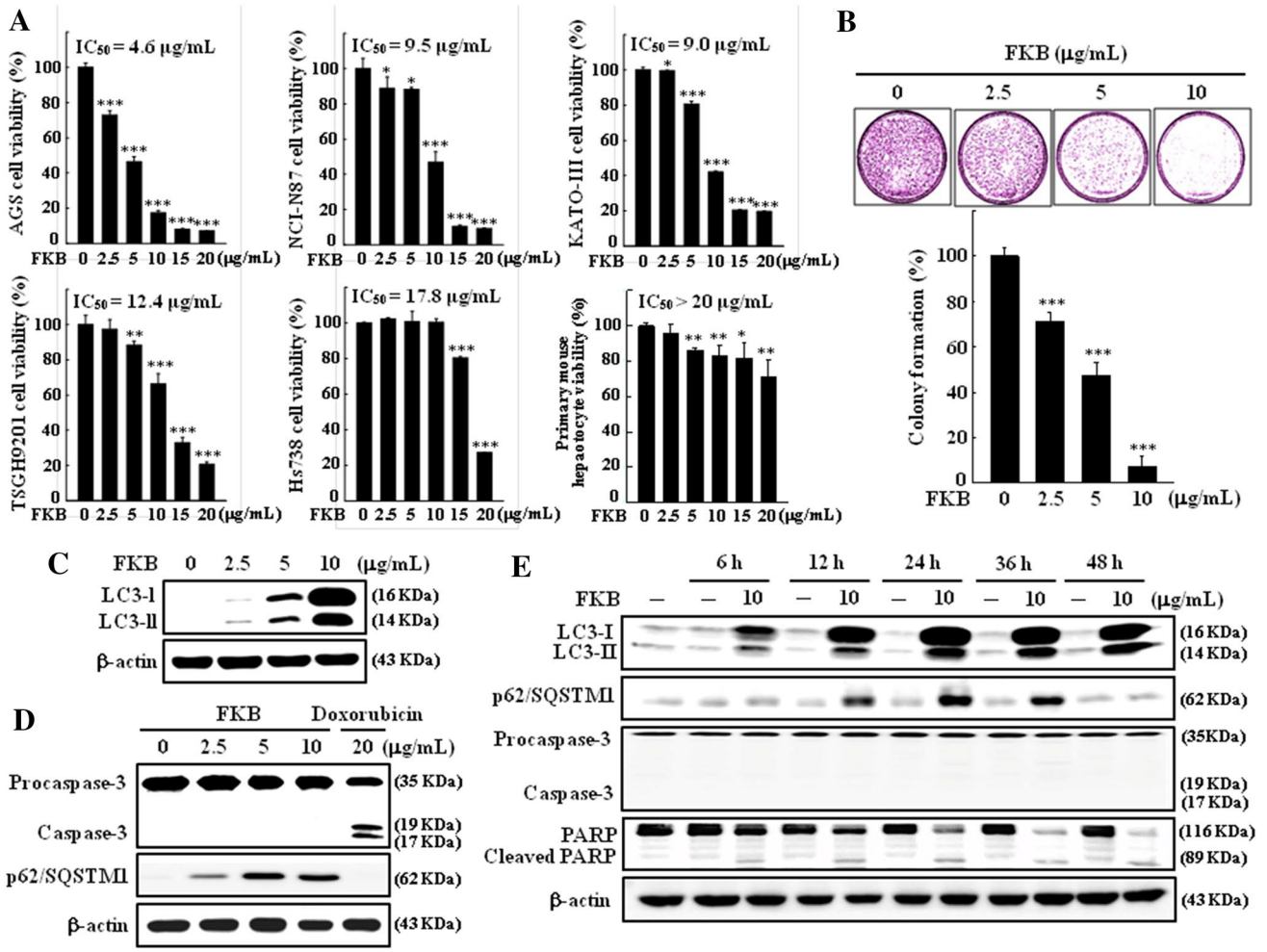

Fig. 1 FKB mediates growth inhibition of gastric carcinoma cells through induction of autophagy. **a** Human gastric carcinoma cells (AGS, NCI-N87, KATO-III, and TSGH9201), normal gastric cells (Hs738), and primary mouse hepatocytes were treated with various concentrations of FKB (0–20 μg/mL) for 24 h. Cell viability was analyzed via MTT assay. **b** FKB inhibits the colony formation ability of AGS cells. Cells were incubated with FKB (0–10 μg/mL) for 7 days, and the percentage of colony formation was calculated by defining the number of colonies in the absence of FKB as 100%. **c** AGS cells were treated with FKB (0–10 μg/mL) for 24 h, and the conversion of LC3-I to LC3-II was determined via Western blot. **d** Changes in caspase-3 and p62/SQSTM1 proteins in response to FKB (0–10 μg/mL) were estimated in AGS cells. **e** AGS cells were incubated with FKB (10 μg/mL), and time-dependent changes in autophagy markers (LC3-I/LC3-II and p62/SQSTM1) and the cleavage of apoptotic proteins (procaspase-3 and PARP) were determined at 6, 12, 24, 36, and 48 h following treatment. Values are expressed as the mean ± SD ($n = 3$). Significant at $^{*}p < 0.05$; $^{**}p < 0.01$; $^{***}p < 0.001$ compared with control cells

decreased following 48 h treatment with FKB. To determine whether FKB-induced cell death is a result of the induction of apoptosis, we monitored the proteolytic cleavage of procaspase-3 and PARP, which are involved in apoptotic signals. We identified interesting results that FKB was unable to promote the cleavage of procaspase-3 and PARP with increasing concentrations (0–10 μg/mL) or incubation times (0–48 h) of FKB in AGS cells (Fig. 1d, e); in contrast, doxorubicin (20 μg/mL), an apoptosis inducer, cleaved procaspase-3 compared with the control (Fig. 1d). These findings indicate that FKB activates the autophagic pathway in gastric carcinoma cells, but not apoptosis.

FKB activates autophagy signaling cascades as a death mechanism in AGS cells

To further confirm that FKB-induced autophagic LC3-II accumulation, GFP-LC3 plasmid was transiently transfected into AGS cells, and the conversion of GFP-LC3 and endogenous LC3 levels were determined via confocal microscopy and Western blot analyses, respectively. The

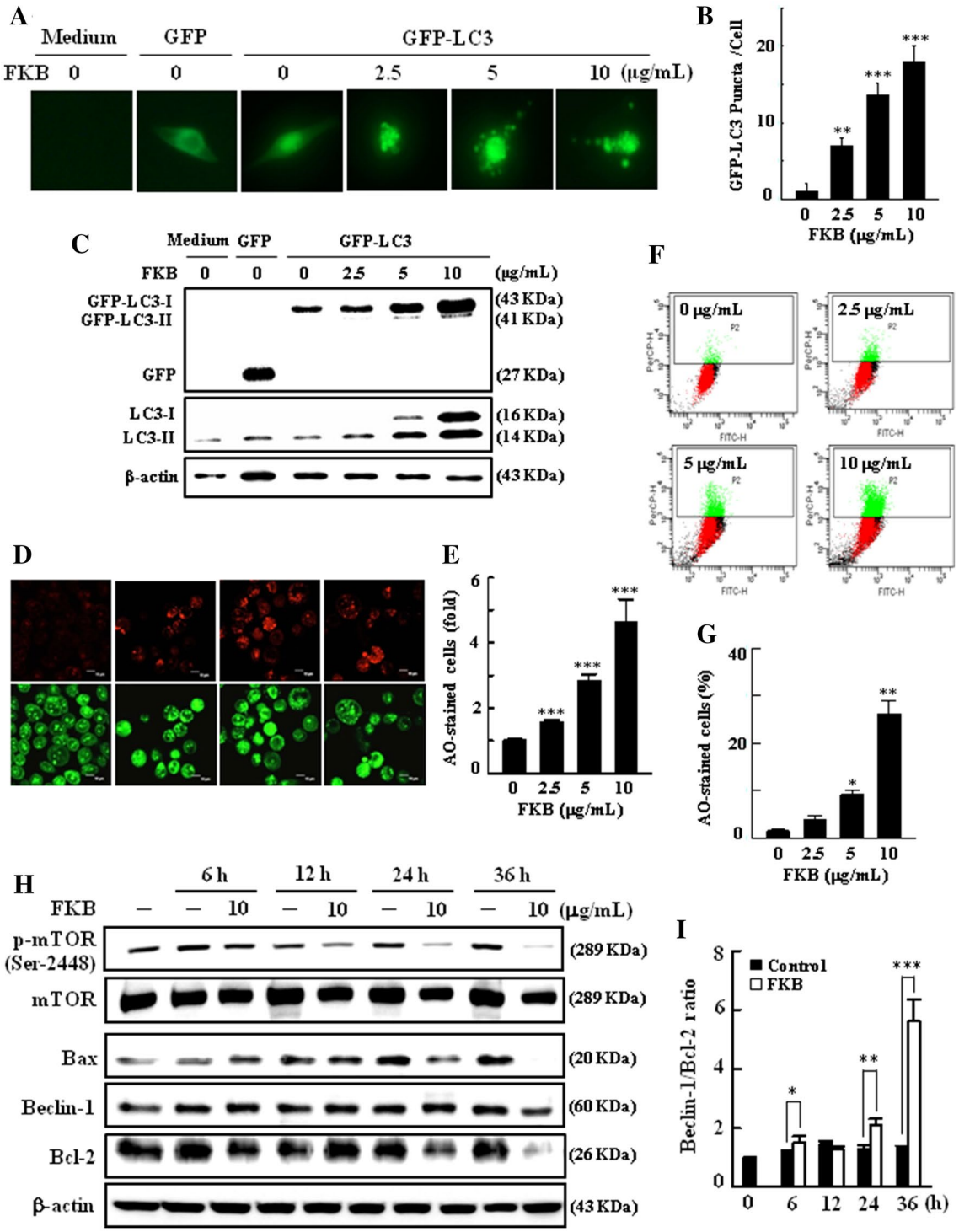

FKB-treated (2.5–10 μg/mL) cells exhibited a cornucopia of green LC3 punctate dots in the cytoplasm (Fig. 2a). Both the percentage of cells with GFP-LC3 dots and the average number of GFP-LC3 dots per cell were increased in a dose-dependent manner (Fig. 2b). The formation of AVOs is a typical characteristic of autophagy, which is represented by an increased accumulation of lipidated LC3 levels (Fig. 2c). An increased LC3 accumulation was strikingly demonstrated in the FKB-treated cancer cells; thus, the sequential effect of FKB on AVO formation was detected via fluorescence microscopy and flow cytometry using AO staining (Fig. 2d–g). We demonstrated that the appearance of AVOs (red fluorescence) after FKB treatment (2.5–10 μg/mL, 24 h) was significantly and dose-dependently increased in

◂**Fig. 2** FKB enhances autophagy as a death mechanism in human gastric cancer (AGS) cells. **a** Cells transfected with GFP-LC3 expression vector were subsequently treated with FKB (0–10 μg/mL) for 24 h. The GFP-LC3 dots induced by FKB were observed with a confocal microscope. **b** Quantification of cells developing GFP-LC3 puncta presented as a histogram. **c** Conversions of GFP-LC3 and endogenous LC3 were also determined via Western blot. **d–g** Acridine orange (AO) was used to stain the AVOs in FKB (0–10 μg/mL)-treated cells for 24 h. **d** Cells were visualized under a red filter fluorescence microscope (×100 magnification). The red fluorescence intensity (in lysosomes) is proportionate to the number of AVOs in cells. **e** Quantification of cells developing AVOs presented as a histogram. The percentage of developed AVOs was calculated based on the results of a fluorescence-activated cell sorting assay. **f** Cells were read flow cytometrically and **g** quantification of cells developing AVOs presented as a histogram. **h** FKB triggers autophagy signaling molecules and downregulates apoptotic Bax proteins. Cells were treated with FKB (10 μg/mL) for 0–36 h, and time-dependent changes in p-mTOR, mTOR, Bax, Beclin-1 and Bcl-2 were monitored via Western blot. **i** Relative changes in the ratio of Beclin-1/Bcl-2 were measured using commercially available quantitative software with the control represented as onefold. Values are expressed as the mean ± SD ($n = 3$). Significant at $^{*}p < 0.05$; $^{**}p < 0.01$; $^{***}p < 0.001$ compared with control cells

the AGS cells in a similar fashion to LC3-II accumulation. These data indicate that FKB-induced autophagic flux in gastric cancer cells.

mTOR signaling is considered a key negative regulator of autophagy; thus, we investigated whether the phosphorylation of mTOR was involved in FKB-induced autophagy. Western blot data demonstrated that FKB treatment substantially inhibited the phosphorylated mTOR (S2448) levels in a time-dependent (0–36 h) manner (Fig. 2h). These results conferred that FKB activates autophagy through the inhibition of mTOR signaling molecules in gastric cancer cells.

FKB dysregulates Beclin-1 and Bcl-2 ratio

The Bcl-2 family proteins are critical regulators of mitochondrial-mediated apoptotic induction and act as activators (Bax) or inhibitors (Bcl-2) (Thiyagarajan et al. 2015). The interaction between the anti-apoptotic protein Bcl-2 and the autophagy protein Beclin-1 is complex. Bcl-2 has been reported to reduce the pro-autophagic property of Beclin-1, whereas Beclin-1 cannot neutralize the apoptotic function of Bcl-2 (Kang et al. 2011). Therefore, we investigated the effect of FKB on Bcl-2 protein and its role with respect to Bax (pro-apoptotic) and Beclin-1 (pro-autophagic) expressions in AGS cells. The results demonstrated that both Bcl-2 and Bax proteins were substantially decreased with FKB in a time-dependent (0–36 h) manner (Fig. 2h). FKB treatment did not change the Beclin-1 expression, whereas it decreased the Bcl-2 expression. There is a significantly increased Beclin-1/Bcl-2 ratio (Fig. 2i), which indicated that the dysregulation of the Beclin-1 and Bcl-2 ratio in the presence of FKB may tip the homeostasis towards autophagy and not apoptosis in AGS cells.

FKB-induced AGS cytotoxicity does not occur through apoptosis

Caspases are typically in an inactive form, and their activation plays a crucial role in the execution phase of apoptosis. Caspases are synthesized in cells as inactive precursors or pro-caspases, which are typically activated by cleavage and propagate the apoptotic pathways. To determine whether FKB activates apoptotic or autophagic signals, we pre-treated cells with apoptosis or autophagy inhibitors, and we determined the changes in the morphology, protein levels, and viability. We demonstrated that the inhibition of caspase activation by Z-VAD-FMK diminished the FKB-induced dramatic alteration in the membrane morphology of AGS cells (Fig. 3a). Western blot data demonstrated that Z-VAD-FMK pre-treatment did not exhibit a significant change in the expressions of LC3-I/LC3-II, p62/SQSTM1 or caspase-3 proteins against the FKB effect (Fig. 3a). Furthermore, the FKB-induced notable cell death of AGS cells was not attenuated in the presence of the apoptosis inhibitor. Not surprisingly, the treatment of AGS cells with Z-VAD-FMK recovers doxorubicin-induced apoptosis. These results suggest that FKB-induced cell death may not link with apoptotic pathways in AGS cells (Fig. 3b).

We subsequently determined the autophagy flux in cells via treatment with autophagy inhibitors, CQ or 3-MA, which inhibit late or early autophagy, respectively. The cells treated with late autophagy inhibitor CQ plus FKB exhibited a greater increase in the LC3-II accumulation, which was prominent compared with the FKB alone-induced elevation (Fig. 3c). In contrast, the cells treated with 3-MA plus FKB diminished the FKB-induced LC3-II accumulation in AGS cells (Fig. 3e). Regardless of their divergent effects on LC3-II accumulation, both inhibitors, CQ and early autophagy inhibitor 3-MA, significantly reversed the FKB-induced cell death of AGS cells (Fig. 3d, f). These results support the notion that the activation of autophagic pathways by FKB may contribute to gastric cancer cell death, and this phenomenon is apoptosis-independent.

FKB inhibits ROS-related ATG4B in AGS cells

We further demonstrated that FKB treatment significantly decreased the ATG4B expression in a dose- and time-dependent manner in the AGS cells compared with the control (Fig. 3g). To determine the role of ROS in ATG4B-mediated activation of the autophagic pathway, we determined the ATG4B protein expression via treatment of AGS cells with FKB and ROS inhibitors (NAC). Interestingly,

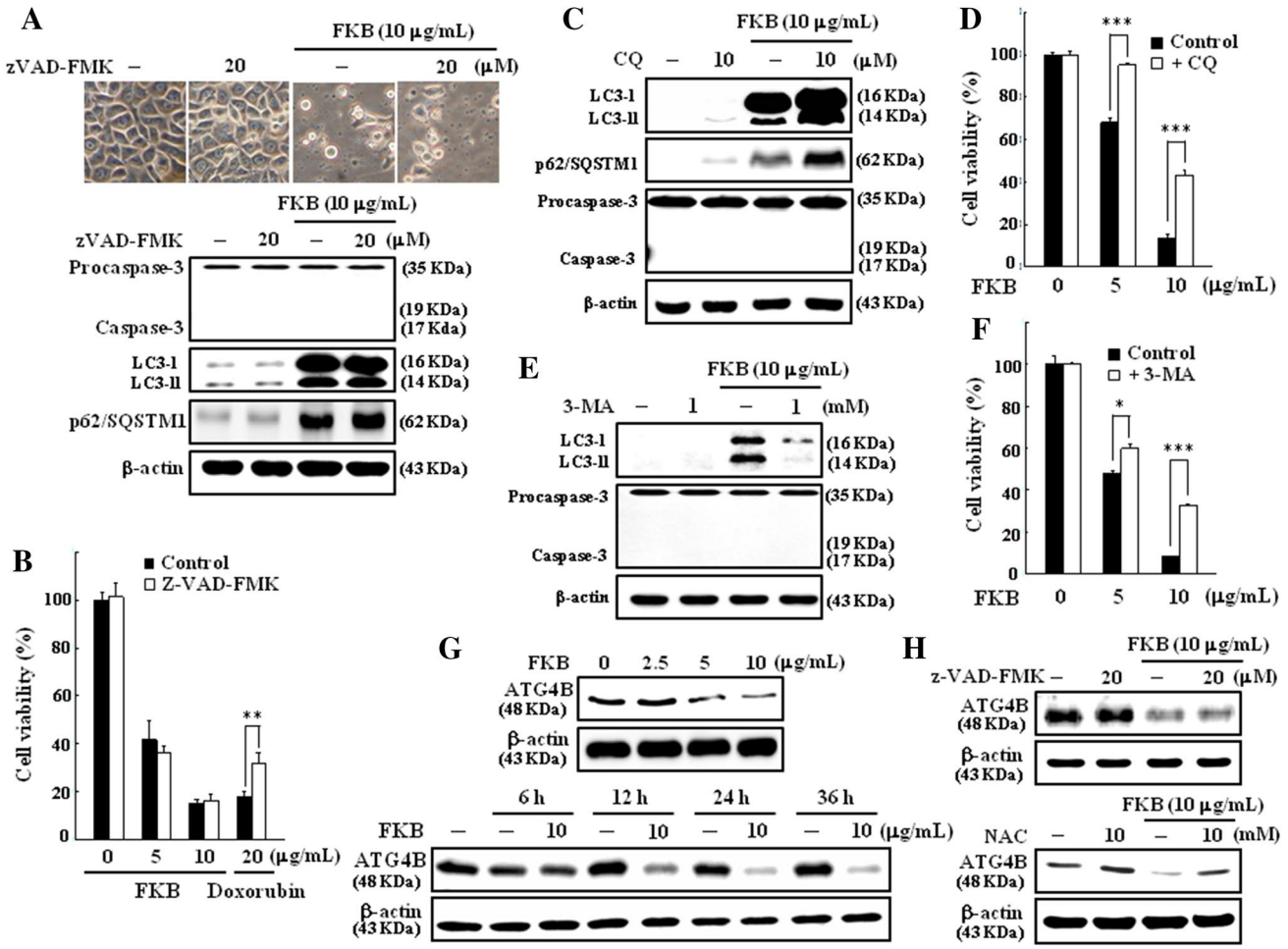

Fig. 3 FKB induces cell death via autophagic pathways, not apoptotic pathways, in AGS cells. **a–h** Cells were pre-treated with caspase inhibitor Z-VAD-FMK (20 μM) **(a, b)** or autophagy inhibitors CQ (10 μM) **(c, d)** and 3-MA (1 mM) **(e, f)** for 1 h followed by FKB incubation (10 μg/mL) for 24 h. Morphological changes following FKB treatment were observed in the presence or absence of Z-VAD-FMK using phase contrast microscopy (×200 magnification). Changes in the expressions of LC3-I/II, p62/SQSTM1 and caspase-3 were monitored via Western blot. **b, d, f** Cell viability was determined via MTT assay. Doxorubicin (20 μg/mL) was used as an apoptosis inducer. Values are expressed as the mean ± SD ($n = 3$). Significant at $^{*}p < 0.05$; $^{**}p < 0.01$; $^{***}p < 0.001$ compared with control cells. **g–h** FKB downregulates ATG4B expression. Cells were treated with ROS inhibitor (NAC, 10 mM) or caspase inhibitor Z-VAD-FMK (20 μM) for 1 h prior to FKB treatment (10 μg/mL) for 0–36 h. The expressions of ATG4B were monitored via Western blot

NAC pre-treatment substantially attenuated the FKB-induced loss of the ATG4B levels (Fig. 3h). However, the cells treated with a caspase inhibitor (Z-VAD-FMK) prior to FKB exhibited no effect on the ATG4B expression (Fig. 3h). These results provide novel insights that ROS may play a critical role in the regulation of ATG4B levels in AGS cells.

FKB induces ROS-mediated autophagy in AGS cells

ROS generation has been implicated as an early event in autophagy. To determine whether FKB-induced autophagy is ROS dependent, AGS cells were incubated with an ROS inhibitor (NAC, 10 mM) 1 h prior to FKB treatment (10 μg/mL), and the autophagy markers were determined. As expected, FKB-induced intracellular ROS generation in the AGS cells, and NAC pre-treatment inhibited the ROS generation (Fig. 4a, b). Furthermore, the FKB-induced cell death (Fig. 4c), GFP-LC3 puncta formation (Fig. 4d–f), and AVO formation (Fig. 4g, h) were significantly attenuated by NAC pre-treatment. Western blot results demonstrated that the pre-incubation of cells with NAC caused a significant decrease in the FKB-induced LC-3I/II and p62/SQSTM1 expression (Fig. 4i). Similarly, FKB decreased Beclin-1/Bcl-2 dysregulation was substantially prevented by the NAC pre-treatment (Fig. 4j). Furthermore, FKB-induced downregulation of Bax was not identified in the presence of NAC (Fig. 4j). These results suggest that ROS may be

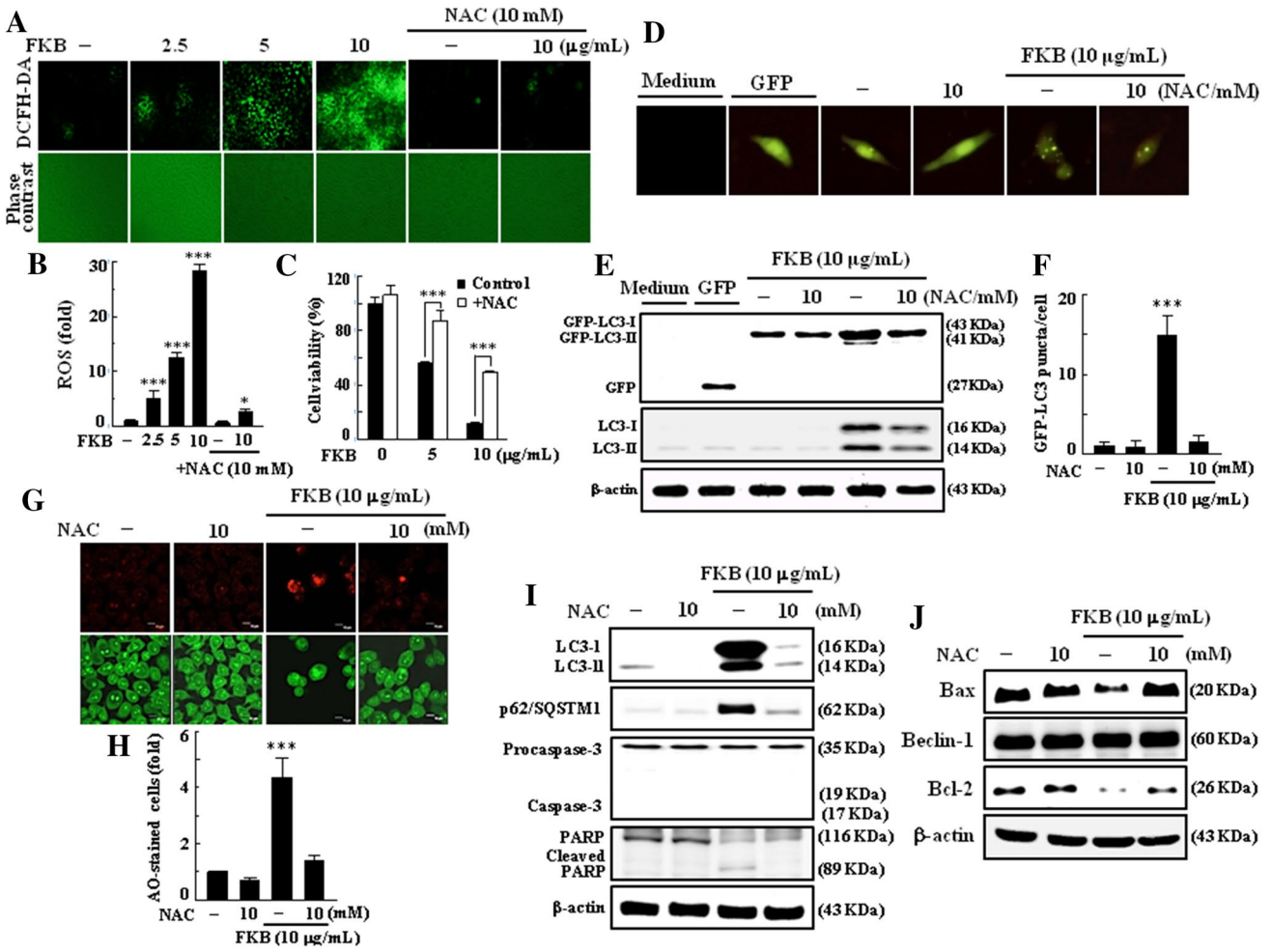

Fig. 4 FKB triggers ROS-mediated autophagy in AGS cells. **a** FKB triggers intracellular ROS generation. AGS cells were treated with FKB (0–10 μg/mL), and ROS generation was measured at 15 min in the presence or absence of a ROS inhibitor (10 mM NAC, 1 h prior to FKB). The non-fluorescent probe $DCFH_2$-DA reacts with cellular ROS and is metabolized into fluorescent DCF, which is proportionate to ROS production. **b** ROS levels are expressed in the graph as a fold of the control. **c** Cell viability was assayed via MTT assay following FKB treatment in the presence or absence of a ROS inhibitor. **d–i** FKB-induced autophagy diminished by NAC. Cells were pre-treated with a ROS inhibitor (NAC, 10 mM) for 1 h and incubated with FKB (10 μg/mL) for 24 h. **d** GFP-LC3 dots were observed using a confocal microscope, and **e** conversions of GFP-LC3 and endogenous LC3 were determined via Western blot. **f** Quantified GFP-LC3 puncta presented as a histogram. **g** AVO formation was visualized using a red filter fluorescence microscope (×100 magnification). **h** Quantification of AVO formation. **i** Expressions of LC3-I/II, p62/SQSTM1, caspase-3 and PARP were monitored via Western blot. **j** Changes in Bax, Beclin-1 and Bcl-2 expressions were determined via Western blot. Values are expressed as the mean ± SD ($n = 3$). Significant at $^*p < 0.05$; $^{***}p < 0.001$ compared with control cells

involved in FKB-induced autophagic-cell death in human gastric carcinoma AGS cells.

To further confirm the role of ROS in FKB-mediated cell death, AGS cells were pre-incubated with ROS modulators for 1 h, followed by FKB treatment for 24 h. The results demonstrated that catalase, vitamin C, and Trolox (scavengers of H_2O_2 and ROS, respectively) effectively reversed the FKB-induced cell death (Fig. 5a–c), which indicates that ROS play a vital role in the growth inhibitory effect of FKB. Apocynin (an inhibitor of NADPH dehydrogenase) and buthionine sulfoximine (BSO, an inhibitor of glutathione synthesis) did not provide protection against FKB-induced cell death (Fig. 5d, e). Nevertheless, the pre-treatment of cells with both the intra and extracellular Ca^{2+}-chelators EGTA and BAPTA (calcium influx and intracellular calcium overload) partially inhibited the FKB-induced cell death (Fig. 5f); these results indicate that FKB-induced changes in Ca^{2+}-homeostasis may be one pathway for the FKB induction of ROS and cytotoxicity.

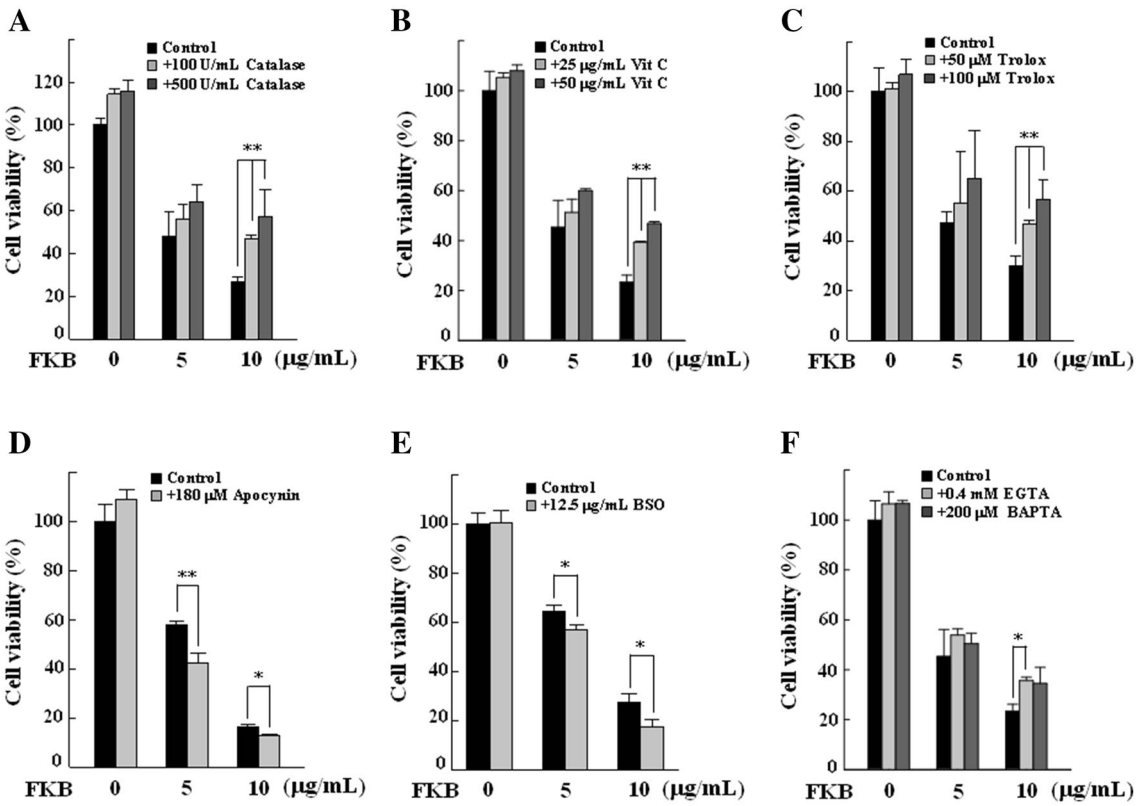

Fig. 5 Effects of ROS modulators on FKB-induced AGS cell death. **a–f** Cells were treated with catalase (100 and 500 U/mL), vitamin C (25 and 50 μg/mL), Trolox (50 and 100 μM), apocynin (180 μM), BSO (12.5 μg/mL), EGTA (0.4 mM), and BAPTA (200 μM) for 1 h prior to FKB treatment (0, 5 or 10 μg/mL) for 24 h. Cell viability was assayed via MTT assay. Values are expressed as the mean ± SD ($n = 3$). Significant at $^{*}p < 0.05$; $^{**}p < 0.01$ compared with untreated control cells at respective doses

FKB induces both autophagy and apoptosis in gastric cancer NCI-N87 cells

We subsequently examined the type of cell death mediated by FKB in NCI-N87 cells by measuring the key molecular proteins. We identified a concentration-dependent increase in the LC3-I/II expression following FKB treatment for 24 h. Furthermore, FKB treatment enhanced the proteolytic cleavage of procaspase-3 and PARP in the NCI-N87 cells (Fig. 6a). The pre-treatment of NCI-N87 cells with an apoptosis inhibitor (Z-VAD-FMK) and autophagy inhibitors (CQ or 3-MA) significantly diminished the FKB-induced cell death (Fig. 6b). These results suggest the coexistence of both apoptotic- and autophagic-cell death in NCI-N87 cells following FKB treatment.

Bax-transfected AGS cells promote both apoptosis and autophagy by FKB treatment

We investigated the effect of FKB on changes in the pro-apoptotic (Bax), pro-autophagic (Beclin-1) and anti-apoptotic (Bcl-2) protein expressions in NCI-N87 and AGS cells. FKB treatment for 24 h suppressed the Bax expression in the AGS cells, whereas it enhanced the expression in the NCI-N87 cells (Fig. 6c). There was no change in the Beclin-1 expression, whereas Bcl-2 was downregulated in both the AGS and NCI-N87 cells following FKB treatment (Fig. 6c). These results indicate that Bax activation by FKB may contribute to the induction of apoptosis in gastric cancer cells.

To confirm this phenomenon, AGS cells were transfected with Bax or vector, and changes in both apoptotic and autophagic proteins were determined following FKB treatment. Western blot analysis demonstrated that FKB treatment exhibited an increase in the Bax/Bcl-2 ratio, decrease in the Beclin-1/Bcl-2 ratio, activation of caspase-3, cleavage of PARP, and decrease in LC3-I/II and p62/SQSTM1 expressions in the Bax-transfected AGS cells (Fig. 6d). We also performed a TUNEL assay in Bax-transfected AGS cells. Images obtained using a fluorescent microscope illustrated increased green fluorescent, TUNEL-positive cells in Bax-transfected cells with FKB treatment, which denotes an increased apoptotic DNA fragmentation (Fig. 6e). We subsequently performed a TUNEL assay to determine the apoptotic DNA fragmentation in Bax-transfected AGS cells. Images obtained using a

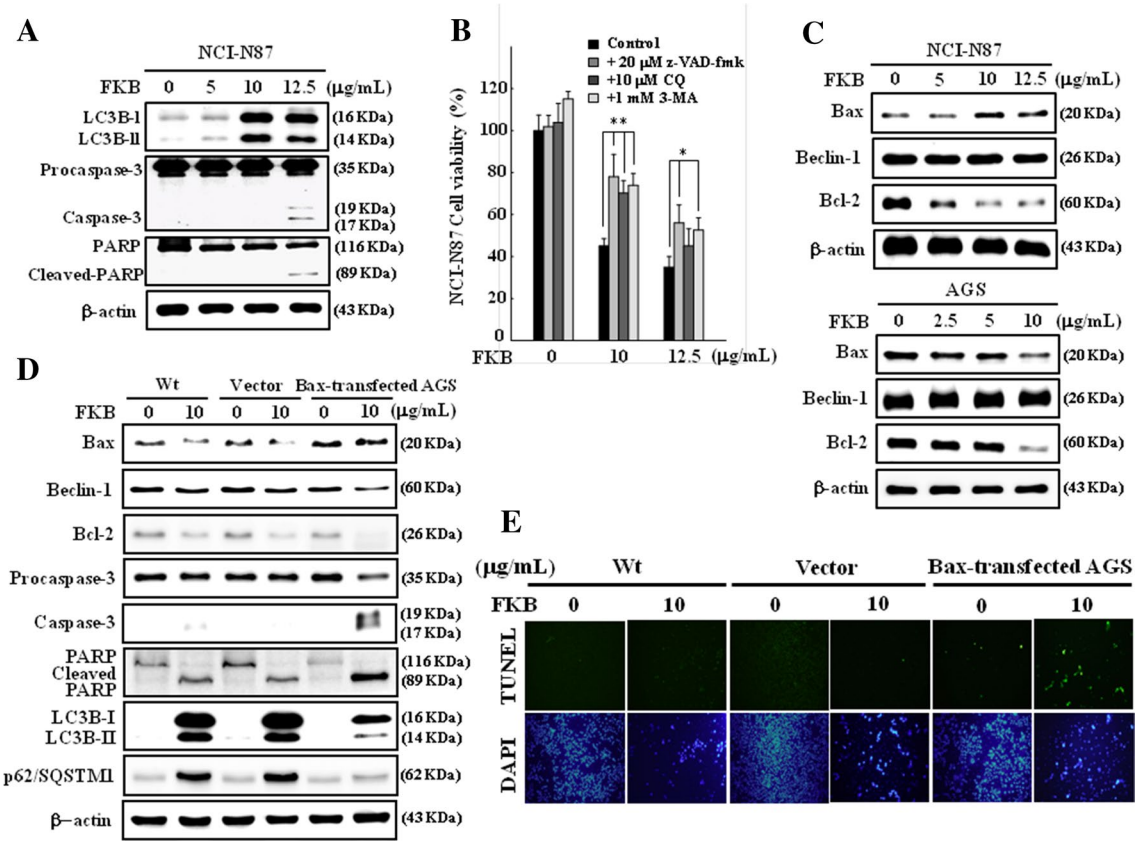

Fig. 6 Bax transfection promotes both apoptosis and autophagy in FKB-treated AGS cells. **a** FKB induces both autophagy and apoptosis in human gastric cancer (NCI-N87) cells. Conversions of LC3-I to LC3-II, cleavage of procaspase-3, and PARP were determined via Western blot in NCI-N87 cells following incubation with FKB (0–12.5 μM) for 24 h. **b** FKB enhances apoptotic- and autophagic-death of NCI-N87 cells. Cells were pre-treated with caspase inhibitor Z-VAD-FMK (20 μM) or autophagy inhibitors CQ (10 μM) and 3-MA (1 mM) for 1 h, followed by FKB treatment (10 or 12.5 μg/mL) for 24 h. Cell viability was determined via MTT assay. **c** FKB upregulates Bax in NCI-N87 cells. Dose-dependent changes in Bax, Beclin-1 and Bcl-2 expressions following FKB treatment (0–12.5 μg/mL) were determined in NCI-N87 and AGS cells. **d, e** Effect of FKB on Bax-transfected AGS cells. Bax-transfected cells were treated with FKB (10 μg/mL) for 24 h. **d** Changes in the expressions of Bax, Beclin-1, Bcl-2, caspase-3, PARP, LC3-I/II and p62/SQSTM1 proteins were monitored via Western blot. **e** Apoptotic DNA fragmentation was determined via TUNEL assay. Green florescence indicates TUNEL-positive cells in the microscopic fields (×200 magnification) from three separate samples. Values are expressed as the mean ± SD ($n = 3$). Significant at $^{*}p < 0.05$; $^{**}p < 0.01$ compared with untreated control cells at respective doses

fluorescent microscope illustrated the increased green fluorescence (TUNEL-positive cells), which denotes increased apoptosis with Bax transfection following FKB treatment (Fig. 6e). Collectively, these results indicate that Bax transfection promotes both apoptosis and autophagy, and Bax inactivation results in apoptosis inhibition in FKB-treated AGS cells.

FKB upregulates JNK and ERK signaling pathways in AGS Cells

In light of the evidence that MAP kinase family proteins, including JNK, ERK, and p38 MAPK, have critical roles in cell fate (Munshi and Ramesh 2013), the effect of FKB on the expression and activation of MAPKs was examined. AGS cells were pretreated with NAC (10 mM) for 30 min, followed by FKB (10 μg/mL) for 24 h; the changes in the total and phosphorylated JNK, ERK, and p38 levels were subsequently assessed via Western blot. As indicated in Fig. 7a, FKB treatment significantly enhanced the activation of p-JNK and p-ERK proteins; however, it did not change the p-p38 levels. Moreover, changes in p-JNK were abandoned in the presence of an ROS inhibitor (Fig. 7a).

We subsequently determined the effect of MAPKs on cell viability, apoptosis, and autophagy-related proteins. Cells were pre-treated with MAPK inhibitors for JNK (SP600125, 25 μM), ERK (U0126, 20 μM) or p38 (SB203580 or SB202190, 20 μM) for 30 min and then treated with FKB (10 μg/mL) for 24 h. Intriguingly, no significant changes in the expressions of LC3-I/II, PARP, Bax, Beclin-1 or Bcl-2 proteins were identified when the cells were exposed to MAPK inhibitors plus FKB (Fig. 7b).

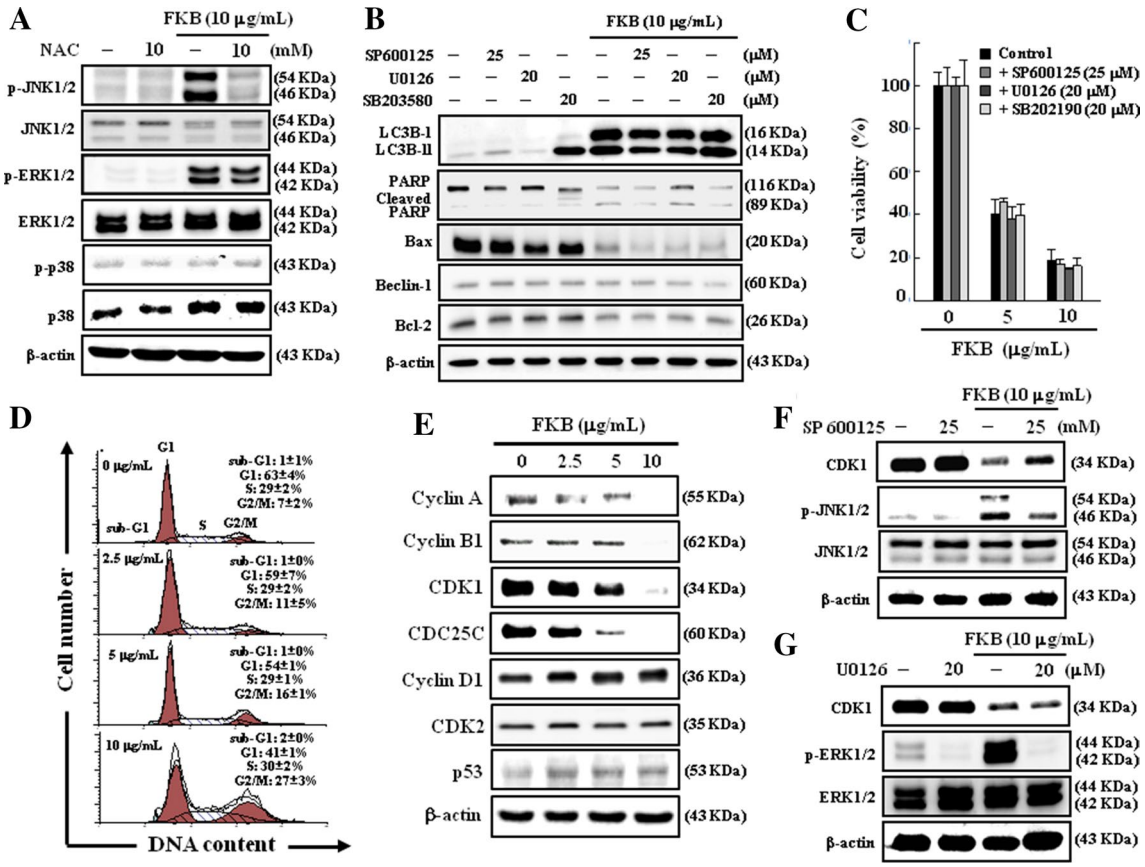

Fig. 7 FKB induces G_2/M arrest through ROS-JNK signaling pathways in AGS cells. **a** FKB activates ROS-JNK signaling pathways. Cells were pre-treated with NAC (10 mM) for 1 h, followed by FKB (10 μg/mL). Total cell lysates were subjected to Western blot with specific antibodies against p-JNK1/2, p-ERK1/2 and p-p38. Total JNK1/2, ERK1/2 and p38 levels were assessed as the loading controls. **b, c** MAPK signaling is not involved in FKB-induced autophagy-death. Cells were pretreated with inhibitors of JNK (SP600125, 25 μM), ERK (U0126, 20 μM) or p38 (SB203580, 20 μM) for 30 min, followed by incubation with FKB (10 μg/mL) for 24 h. **b** Changes in LC3-I/II, PARP, Bax, Beclin-1 and Bcl-2 proteins were analyzed via Western blot. **c** Cell viability was assayed via MTT assay. **d, e** FKB-induced G_2/M arrest. **d** Cells were treated with FKB (0–10 μg/mL) for 24 h, stained with PI and analyzed for cell-cycle phase via flow cytometry. The cellular distribution (percentage) in cell-cycle phases (G_1, S and G_2/M) after FKB treatment is presented. **e** Effects of FKB on cyclin A, cyclin B1, CDK1, CDC25C, cyclin D1, CDK2 and p53 levels were monitored via Western blot. **f, g** FKB-activated JNK signaling pathways involved in G_2/M arrest. Cells treated with JNK inhibitor (SP600125, 25 μM) or ERK inhibitor (U0126, 20 μM) prior to FKB (10 μg/mL) and changes in CDK1 (24 h), p-JNK1/2 (15 min), or p-ERK1/2 (15 min) were detected via Western blot. Values are expressed as the mean ± SD ($n = 3$)

Furthermore, MAPK inhibitors did not exhibit an effect on cell viability (Fig. 7c).

FKB causes G_2/M arrest through ROS-JNK signaling pathways in AGS cells

To determine whether FKB treatment affected the cell-cycle progression of AGS cells, synchronized cells were treated with FKB (2.5–10 μg/mL) for 24 h and subjected to flow cytometric analysis of DNA staining. Figure 7d indicates that FKB exposure resulted in a progressive and sustained accumulation of cells in the G_2/M cell-cycle phase. The formation of a complex between CDK1 and Cyclin A/B1 is an important event for cells to enter mitosis. Therefore, we hypothesized that the FKB-induced G_2/M arrest may be a result of the inhibition of cell-cycle proteins, which are critically involved in G_2/M progression. As expected, FKB (2.5–10 μg/mL) treatment for 24 h caused a significant decrease in the protein levels of Cyclin A, Cyclin B1, CDK1 and CDC25C in a dose-dependent manner, whereas no changes in the Cyclin D1 and CDK2 were identified (Fig. 7e). In addition, FKB treatment significantly increased the p53 protein level in a dose-dependent manner (Fig. 7e).

We subsequently aimed to determine whether pharmacological inhibition of JNK and ERK altered cell-cycle proteins involved in G_2/M arrest. As indicated in Fig. 7f, FKB treatment significantly decreased the CDK1 expression level. However, the pre-treatment of AGS cells with a JNK (SP 600125) inhibitor reversed the FKB-mediated

downregulation of CDK1. In contrast, no significant changes in the CDK1 expression were identified when the cells were exposed to an ERK (U0126) inhibitor (Fig. 7g). In addition, we also demonstrated that the p-JNK activation was abandoned in the presence of an ROS inhibitor (Fig. 7a). Collectively, these data imply that FKB may induce G_2/M arrest through the ROS-JNK signaling pathways and inhibit cell-cycle progression by reducing the levels of cyclin A, cyclin B1, CDK1 and CDC25C in AGS cells.

Inhibitory effects of FKB on PI3K/AKT/mTOR signaling pathway and HER-2 receptor levels in gastric cancer cells

HER-2 overexpression has been demonstrated to aggressively promote PI3K/AKT/mTOR signals, which are responsible for the regulation of various aspects of tumor biology, such as cancer cell invasion, differentiation and survival (Komoto et al. 2009). We demonstrated that FKB treatment significantly inhibited the total and phosphorylated HER-2 levels in AGS cells (Fig. 8a). We subsequently aimed to determine the effect of FKB on downstream signaling proteins, including PI3K, AKT and mTOR. Western blot data demonstrated that FKB treatment significantly and dose-dependently inhibited the total and phosphorylated levels of PI3K, AKT and mTOR in the AGS cells (Fig. 8a). These data suggest that the suppression of HER-2 signaling by FKB treatment resulted in the inhibition of the PI3K/AKT/mTOR signaling cascades. To delineate whether FKB-suppressed HER-2 and PI3K/AKT/mTOR signaling is linked to the activation of autophagy, AGS cells were pre-incubated with late autophagy inhibitor CQ for 1 h and subsequently treated FKB for 24 h. We identified interesting results in which CQ pre-treatment abolished the FKB-induced degradation of HER-2, PI3K, AKT and mTOR expressions in the AGS cells (Fig. 8b).

To further confirm the role of FKB in the activation of autophagy in gastric cancer cells, NCI-N87 cells were treated with FKB, and the changes in the total and phosphorylated HER-2, PI3K, AKT, and mTOR levels were determined via Western blot. FKB treatment caused a similar dose-dependent reduction in the total and phosphorylated levels of HER-2, PI3K, AKT, and mTOR in the NCI-N87 cells (Fig. 8c). These results suggest that FKB-suppressed the HER-2 expression and PI3K/Akt/mTOR signaling pathways through the induction of autophagy in human gastric cancer cells (Fig. 8a–c).

In vivo inhibition of tumor growth by FKB treatment in xenografted nude mice

Nude mice were used to investigate the in vivo effects of FKB on tumor growth. AGS cells were xenografted (subcutaneously) into nude mice. All animals appeared healthy, with no loss of body weight noted during the FKB

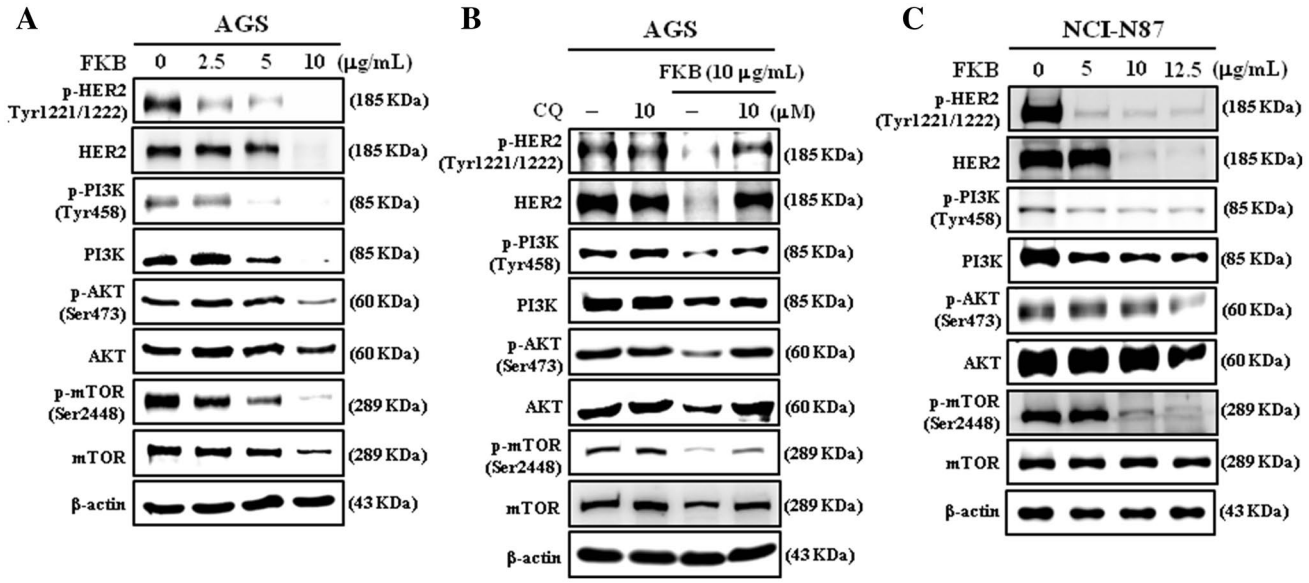

Fig. 8 FKB inhibits phosphorylation of HER-2/*neu*, PI3K/AKT and mTOR in HER-2/*neu*-expressing gastric cancer (AGS and NCI-N87) cells. **a, b** Changes in total and phosphorylated HER-2/*neu*, PI3K, AKT and mTOR in the presence or absence of CQ were monitored via Western blot. **a** AGS cells were incubated with FKB (0–10 μg/mL) for 24 h. **b** AGS cells were pre-incubated with an autophagy inhibitor (CQ, 10 μM) for 1 h and subsequently treated with FKB (10 μg/mL) for 24 h. **c** NCI-N87 cells were treated with FKB (0–12.5 μg/mL) for 24 h; the levels of p-HER-2/*neu*, HER-2/*neu*, p-PI3K/AKT, PI3K/AKT, p-mTOR, and mTOR were determined via Western blot

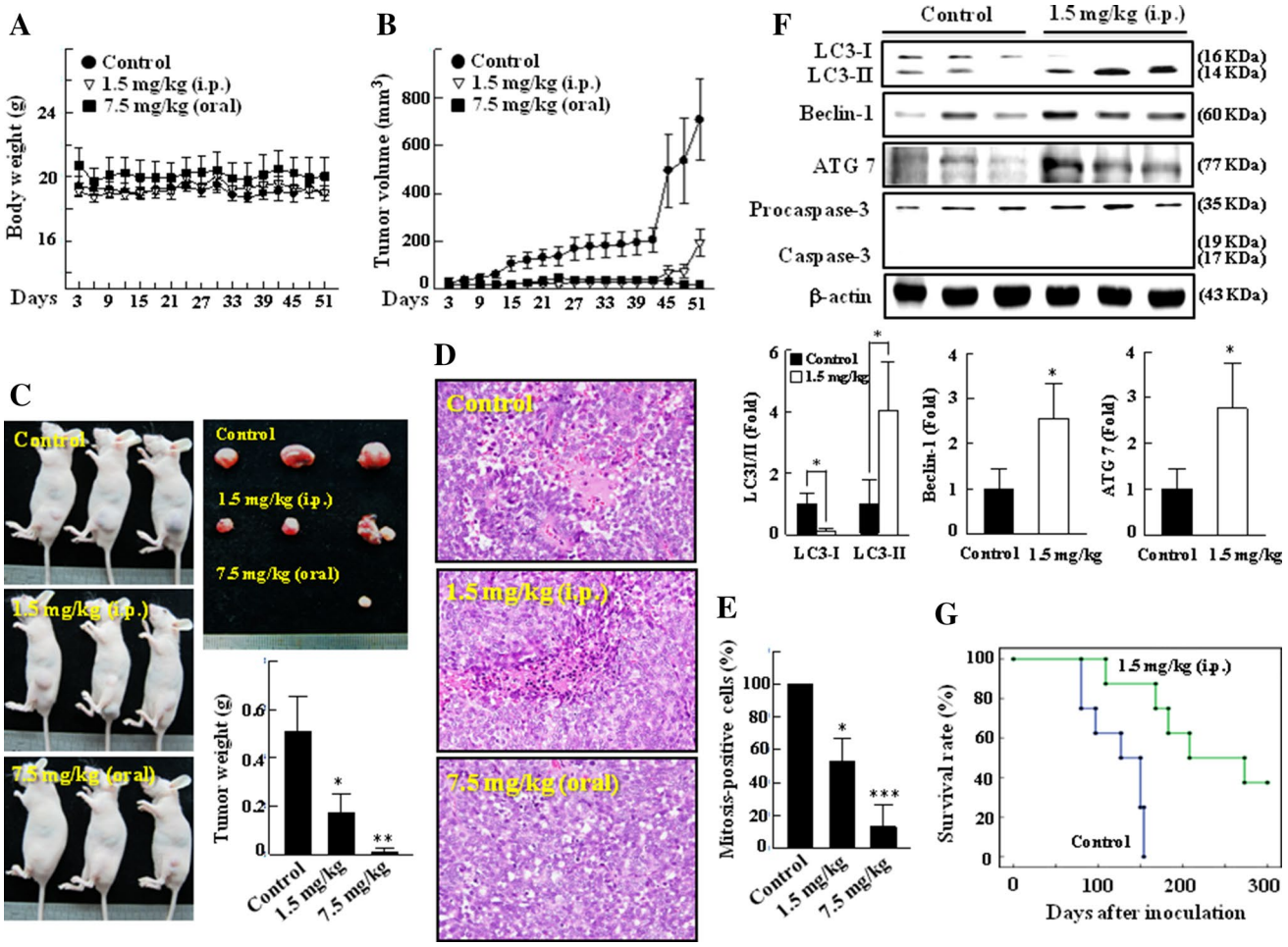

Fig. 9 In vivo inhibition of AGS-xenografted tumors in nude mice by FKB treatment. The body weight **a** and tumor volume **b** were measured every 3 days for 51 days. BALB/c nude mice were treated with vehicle (control), FKB (1.5 mg/kg, intraperitoneal) and FKB (7.5 mg/kg, oral administration) every 2 days until 51 days. **c** On the 51st day after tumor implantation, the animals were photographed and sacrificed, and the tumor tissue was removed and weighed. **d** Xenograft tumors were sectioned, stained with hematoxylin and eosin (H&E), and examined using light microscopy (×400 magnification). The *arrows* indicate mitosis-positive cells. **e** Number of mitosis-positive cells was counted and presented as the percentage of mitosis-positive cells. **f** In vivo autophagy detected via Western blot. Immunoblot data against LC3-I/II, Beclin-1, ATG7 and caspase-3 expressions in xenografted tumors. β-actin was used as a loading control. Relative changes in protein bands were measured via densitometric analysis. The results are presented as the means ± SD ($n = 3$). Significant at $^{*}p < 0.05$; $^{***}p < 0.001$ compared with control group. **g** FKB promotes the animal survival rate. The *curve* indicates the number of mice alive on different days. Data represent 8 FKB-treated and 8 sham-treated mice from day 1 to their natural death

treatment (Fig. 9a). The time course effects of the FKB intraperitoneal (1.5 mg/kg) and oral (7.5 mg/kg) treatments on the AGS-xenografted tumor growth are presented in Fig. 9b. At the end of 51 days, the AGS-xenografted tumor was excised from each sacrificed animal. Tumor volume evaluations indicated that both modes of FKB treatment, intraperitoneal and oral administrations resulted in the inhibition of tumor growth. This phenomenon was more pronounced with the oral administration compared with the intraperitoneal injection (Fig. 9c).

Furthermore, hematoxylin and eosin (H&E) staining of the tumor tissues demonstrated that abundant mitosis was identified in the control group, which indicates proliferating cells, whereas a limited number of mitotic-positive cells were identified in the tumor sections obtained from the FKB-treated (1.5 and 7.5 mg/kg) mice (Fig. 9d, e). Analysis of our data strongly suggests that FKB promoted antitumor activity in nude mice bearing AGS xenografts. The effects of FKB on autophagy and apoptosis-related proteins in the AGS-xenografted mice were also examined in the tumor sections. Western blot analysis demonstrated that FKB treatment significantly increased the LC3I/II, Beclin-1, and ATG7 expressions and caused no caspase-3 activation (Fig. 9f). In addition, the survival ratio was significantly prolonged for the nude mice with FKB treatment compared with the control group (Fig. 9g). These data suggested that

FKB-inhibited AGS tumor development through the induction of an autophagic mechanism.

Silencing of LC3 with shRNA inhibits FKB-induced autophagy in AGS cells

To clarify the role of autophagy in FKB-mediated AGS cell death, an LC3 silencing (shLC3) experiment was performed with a VZV-G pseudotyped lentivirus-shRNA system. As expected, silencing of the LC3 expression failed to convert LC3-I to LC3-II and reduced the p62/SQSTM1 levels, even in the presence of FKB. Furthermore, no effects on the caspase-3 and PARP protein levels were identified by silencing LC3 (Fig. 10a). The FKB-mediated cell viability was subsequently determined in AGS shLuc and shLC3 cells. We demonstrated that the potent cytotoxic effects of FKB were significantly halted in the AGS shLC3 cells (Fig. 10b). Consistent with this finding, the decreased colony formation ability of AGS cells by FKB treatment was substantially reversed following shLC3 transfection. The colony formation ability of AGS shLC3 cells in the presence of FKB is similar to untreated control cells, which emphasizes that the FKB growth inhibitory effect was nullified by LC3 silencing (Fig. 10c, d).

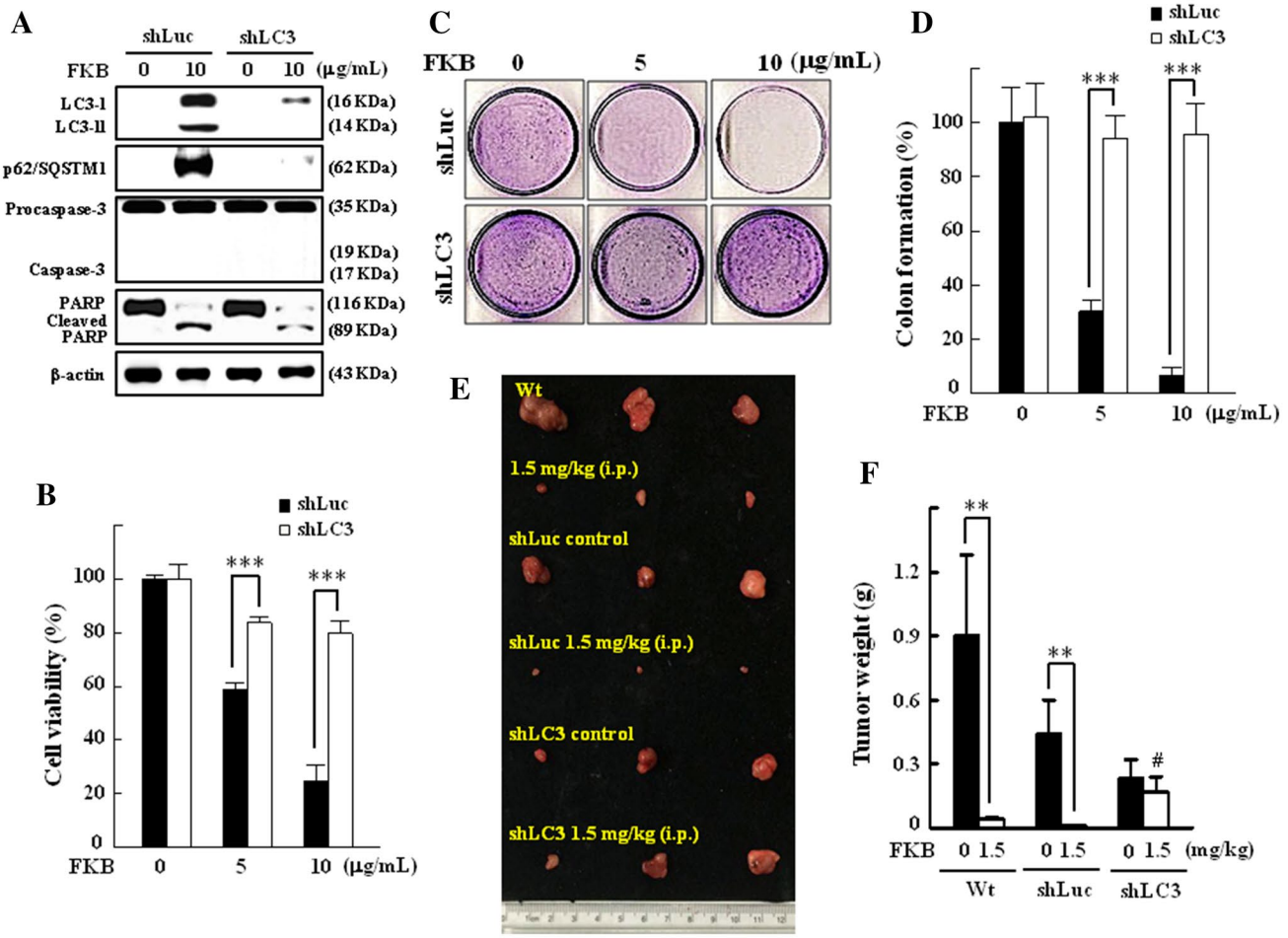

Fig. 10 In vitro or in vivo effects of LC3 silencing on FKB-mediated autophagy. **a, b** AGS shLuc and shLC3 cells were treated with FKB (10 μg/mL) for 24 h. **a** Conversions of LC3-I to LC3-II, p62/SQSTM1, caspase-3 and PARP were determined via Western blot. **b** Cell viability was analyzed via MTT assay. **c** AGS shLuc and shLC3 cells were incubated with FKB (0, 5 or 10 μg/mL) for 7 days, and **d** percentage colony formation was calculated by defining the number of colonies in the absence of FKB as 100%. The results are significant at $^{***}p<0.001$ compared with shLuc cells at respective concentrations of FKB. **(e–f)** In vivo inhibition of AGS shLC3-xenografted tumors in nude mice by FKB. Nude mice were treated with wild type (wt), wt + FKB (1.5 mg/kg, i.p., every 2 days), shLuc control, shLuc + FKB, shLC3 control and shLC3 + FKB. On the 51st day after tumor implantation, the animals were sacrificed, and the tumor tissues were removed and weighed. The results are presented as the means ± SD ($n=3$). Significant at $^{**}p<0.01$ compared with untreated control, $^{\#}p<0.05$ compared with FKB alone treated wild type (Wt) mice

LC3 Silencing attenuates FKB-induced AGS-xenografted tumor growth in mice

We subsequently expanded our studies from cell cultures to animal models. AGS xenografts were further subjected to FKB alone (1.5 mg/kg), shLuc control, shLuc plus FKB, shLC3 control, and shLC3 plus FKB treatment (Fig. 10e, f). The results demonstrated that the FKB treatment alone and the combination of shLuc control plus FKB substantially reduced the tumor size, as indicated in Fig. 10e and f. Interestingly, we demonstrated that the shLC3 plasmid transfection and the combination of shLC3 with FKB treatment maintained a similar tumor volume growth (Fig. 10e, f). This in vivo evidence further indicated that FKB-inhibited tumor growth was reversed by LC3 silencing.

AGS shLC3-xenografted mice attenuated FKB-induced autophagy

To further strengthen our findings that FKB-induced autophagy contributes to the inhibition of tumor growth in vivo, we performed Western blot and immunohistochemical analyses to monitor the changes in autophagy and apoptosis signaling molecules in AGS-xenografted tumor tissues. As indicated in Fig. 11a–d, FKB plus shLuc treatment significantly increased the LC3-II and p62/SQSTM1 expressions; however, no change in caspase-3 was identified. Noteworthy, shLC3 transfection obliterated the FKB-induced upregulation of LC3-II and p62/SQSTM1 expressions in the tumor samples. Furthermore, evidence from the immunohistochemical analysis indicated that FKB plus shLuc significantly increased the LC3-II accumulation in the tumor tissues without affecting the caspase-3 levels. However, shLC3 completely diminished the FKB-induced LC3-II accumulation in the tumor tissues (Fig. 11e). These results were consistent with our in vitro findings and confirmed that the silencing of LC3 attenuated the FKB-induced autophagy in AGS-xenografted mice.

Discussion

Emerging evidence in cancer research emphasizes that the activation of autophagic-cell death is a fundamental episode in the execution of tumor cell death and the management of gastric cancers (Hasima and Ozpolat 2014). Long-term studies have demonstrated that many natural compounds from plant and food sources have chemopreventive and chemotherapeutic efficacies against human cancer (Pan and Ho 2008). Recently, several reports have indicated that the use of dietary bioactive compounds is becoming a safe and salient approach to prevent and treat cancer. Chalcones, one of the major classes of naturally occurring biological compounds has recently received substantial attention for their interesting pharmacological applications (Nowakowska 2007). FKB, a naturally occurring chalcone, has been demonstrated to exhibit a strong cytotoxic potency against human colon (HCT-116), lung adenocarcinoma epithelial (A-549), and prostate (PC3 and DU-145) cell lines (Hseu et al. 2012; Lin et al. 2012). Our previous study demonstrated that FKB isolated from *Alpinia pricei* (shell gingers) exhibits strong anticancer effects via the induction of cell-cycle arrest and apoptosis in human squamous carcinoma KB and oral carcinoma HSC-3 cells (Hseu et al. 2012). *Alpinia* plants possess various biological activities, including antioxidant, anti-inflammatory, anticancer, immunostimulating, hepatoprotective and antinociceptive activities (Hseu et al. 2012). FKB predominantly inhibited the cell viability of gastric carcinoma AGS cells, which suggests its sensitivity towards cancer cells. The present findings emphasized that FKB-induced autophagic-cell death, but not apoptosis, occurred in gastric carcinoma cells and that the autophagy-inducing activity is at least partially related to ROS accumulation.

Kava (*Piper methysticum* Foster, Piperaceae) organic solvent-extract has been used to treat mild to moderate anxiety, insomnia, and muscle fatigue in Western countries, which has led to its emergence as one of the ten bestselling herbal preparations. Several reports of severe hepatotoxicity in kava consumers led the U.S. Food and Drug Administration and authorities in Europe to restrict the sales of kava-containing products (Hseu et al. 2012). However, the long-term treatment of ethanolic kava extracts (73 mg/kg, daily) for 6 months demonstrated no signs of hepatotoxic effects in rats (Sorrentino et al. 2006). Singh and Devkota (2003) determined the cytotoxic effects of aqueous kava extract on liver function in rats (200–500 mg/kg daily) for up to 4 weeks and determined there were no changes in the ALT, AST, ALP or LDH levels (Singh and Devkota 2003). A study by Clayton and colleagues examined the toxicological effects of organic kava extract with various concentrations that ranged from 0.25 to 2 g/kg/day in rats (Clayton et al. 2007). Time- and dose-dependency studies indicated there were no hepatotoxic effects with a dose of 0.25 g/kg/day. A toxicity level of 1 g/kg/day appeared after 93 days of treatment, whereas a toxicity level of 2 g/kg/day was identified only 4 days after treatment (Clayton et al. 2007). Another rat study demonstrated that the ethanolic and acetonic extracts of kava at three different oral doses (31.25, 62.5 and 133 mg/kg diet) did not cause liver injury based on serum markers of liver damage and serum lipid peroxides (DiSilvestro et al. 2007). In accordance with previous reports, FKB (chalcone) exhibited less cytotoxicity towards human normal (Hs738) cells and normal primary mouse hepatocytes. However, FKB produced potent cytotoxic effects towards cancer cells, in which

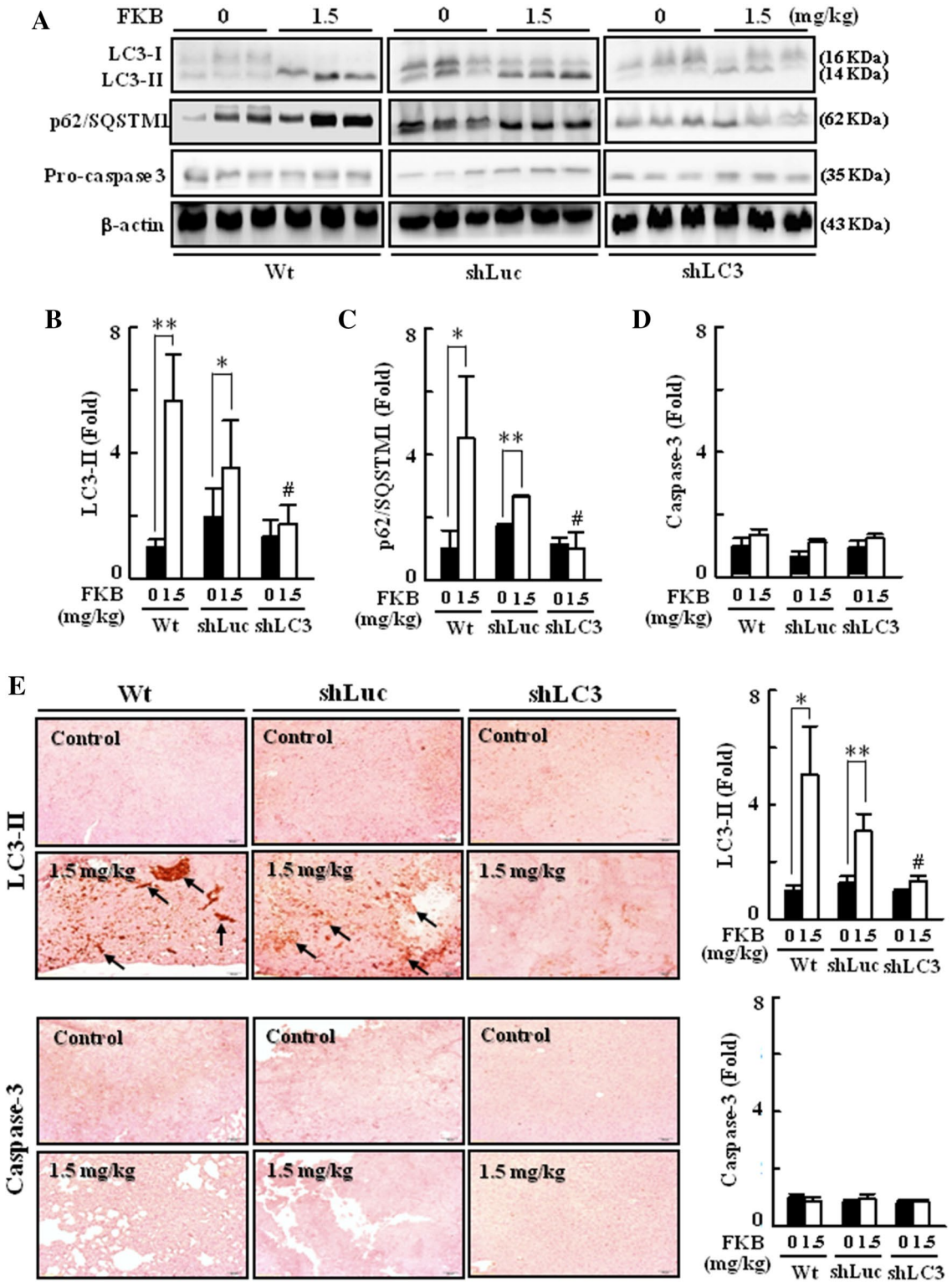

Fig. 11 Western blot and histochemical analyses of autophagy in AGS shLC3-xenografted tumors. Western blot and immunohistochemical analyses were performed in AGS-xenografted tumors following shLC3 transfection in the presence or absence of FKB (1.5 mg/kg, i.p., every 2 days). **a** Expressions of LC3-I/II, p62/SQSTM1 and caspase-3 in tumors were determined via Western blot. β-actin was used as a loading control. **b–d** Relative changes in protein intensities were quantified via densitometric analysis and presented as histograms. **e** Xenografted tumor sections were subjected to immunohistochemical analysis for the detection of LC3-II and caspase-3 expressions using light microscopy (×400 magnification). *Arrows* indicate LC3-II positive cells. The results are presented as the means ± SD ($n = 3$). Significant at $^{*}p < 0.05$; $^{**}p < 0.01$ compared with untreated control mice, $^{\#}p < 0.05$ compared with FKB alone treated wild type (Wt) mice

we identified a remarkable death of human gastric cancer (AGS, NCI-N87, KATO-III and TSGH9201) cells followed by micro-molar concentrations of FKB treatment. Our findings are different from a previous study, which suggests FKB is a potent hepatocellular toxin that induces the death of human hepatocyte L-02 (LD_{50} = 32 μM) and hepatoma HepG2 (LD_{50} = 15.3 μM) cells (Zhou et al. 2010). Moreover, FKB treatment has been reported to be safe; however, it significantly enhanced acetaminophen (APAP)-induced hepatotoxicity in C57BL/6 mice (Narayanapillai et al. 2014). Thus, our results indicate that FKB is non-cytotoxic and safe to human normal cells and primary mouse liver cells, but that it is cytotoxic to gastric cancer cells. These findings represent a promising anticancer property of FKB that may be used for the prevention and treatment of human gastric cancer.

Apoptosis and necrosis are well-established mechanisms of cell death induced by anticancer therapies, whereas autophagy-mediated cell death is a relatively recent discovery. Autophagy is a type of caspase-independent cell death that does not involve DNA laddering and that is extensively a result of autophagic degradation of intracellular contents (Ozpolat et al. 2012). Recent studies have provided increasing evidence that natural products may trigger both apoptotic- and autophagic-cell death in several cancers (Hasima and Ozpolat 2014). FKB exhibited a potent cytotoxicity towards human gastric cancer cells; therefore, we determined whether FKB-mediated cell death is dependent on the induction of autophagy or apoptosis. PARP-specific proteolytic cleavage by caspase-3 is considered a biochemical characteristic of apoptosis. Interestingly, FKB treatment did not exhibit caspase-3 activation and PARP cleavage in AGS cells. During autophagosome formation, LC3-I was converted to LC3-II via lipidation by ubiquitin-like conjugation (Tanida et al. 2004). The expression ratio of LC3-I to LC3-II provides a simple indicator for autophagy and has been widely used as an autophagic marker. The current results indicated that FKB-induced AVO staining, punctate staining dots for LC3-II, and an increased protein expression ratio of LC3-II/LC3-I suggest that FKB caused autophagy in AGS cells. Furthermore, pre-treatment with 3-MA/CQ, early or late autophagy inhibitors reversed FKB-induced cell death. These results imply that FKB-induced cell death is mediated by autophagy instead of apoptosis in AGS cells.

The precise molecular mechanism of autophagy remains unclear; however, increasing evidence has suggested that ROS may function as molecular signals to mediate the initiation of autophagy (Pelicano et al. 2004). ROS are highly reactive molecules that have a single unpaired electron in their outermost shell of electrons. ROS, specifically superoxide anion ($O_2^{\cdot -}$) and hydrogen peroxide (H_2O_2), have been reported to induce autophagy (Karna et al. 2010). ROS have been demonstrated to trigger oxidative stress in various organisms. When oxidative stress is induced, cells are able to maintain a state of redox homeostasis. Dysregulations in ROS levels and autophagy play important roles in cancer progression and initiation and have been recognized as potential targets for cancer treatment (Hale et al. 2013). Our present data demonstrated that FKB treatment significantly induced DCF fluorescence in AGS cells, which suggests an increase in intracellular ROS generation. NAC pre-treatment substantially attenuated FKB-induced GFP-LC3 puncta formation and LC3-II expression. Furthermore, cells pre-incubated with ROS modulators significantly reversed FKB-induced autophagic-cell death, which suggested that ROS-mediated FKB-induced autophagy and subsequent cell death.

ATG4B plays an important role in the ATG8/LC3 conjugation system, which is essential for the formation of autophagosomes. Decreased ROS levels result in the hyperactivation of the cysteine endopeptidase ATG4B, which leads to the delipidation of LC3 and defective autophagosome assembly (Qiao et al. 2015). In addition, the knockdown of ATG4B expression has been associated with a decrease in the cell viability and proliferation of chronic myeloid leukemia cells, which leads to an accumulation of LC3-II and p62 expression (Rothe et al. 2014). To corroborate these findings, we analyzed the ATG4B protein expression by treating the cells with FKB and NAC in AGS cells. Our data demonstrated that FKB treatment triggered the intracellular ROS generation, reduced the ATG4B activity, and increased the autophagic capacity. Pre-treatment of NAC attenuated FKB–enhanced intracellular ROS and restored the ATG4B activity, which mitigated FKB–induced autophagy. These observations indicate that FKB may increase intracellular ROS, which leads to the oxidation and inhibition of ATG4B and ultimately promotes the lipidation of LC3 (ATG8) and induction of autophagy. However, further investigation is necessary to extrapolate the specific mechanism of action.

Mitogen-activated protein kinases (MAPKs), including ERK, JNK and p38 MAPK, are a family of serine/threonine kinases that play important roles in the regulation of the cell cycle, apoptosis and tumorigenesis (Zhang et al. 2013). ROS are involved in the regulation of MAPK activation in various stress conditions. p38 MAPK has recently received attention as a tumor suppresser that is activated following cellular stress and often engages pathways that may block proliferation or promote apoptosis (Wagner and Nebreda 2009). In our study, FKB treatment in gastric cancer cells did not lead to a significant change in the total and phosphorylated levels of p38 MAPK. However, the pre-treatment of AGS cells with an ROS inhibitor prevented FKB-induced phosphorylation of JNK and ERK. These results indicate that FKB activates the ERK and JNK

signaling pathways through the activation of ROS generation in human gastric carcinoma cells.

Progression of the cell cycle is tightly controlled through the actions of cyclin-dependent protein kinases. The G2/M transition is predominately dependent on the cyclin B1/CDK1 activity (Zhao et al. 2013). p53 regulates the G2/M transition through the induction of p21. Our findings demonstrated that FKB treatment in AGS cells induced G2/M phase arrest and decreased the cyclin A and cyclin B protein levels with a concomitant decrease in the kinase CDK1 activity. In addition, FKB suppressed the CDK1 activity through the downregulation of CDC25C, which thus controlled the entry of cells into mitosis by maintaining the G_2/M transition phase. These data indicated that FKB-induced G_2/M arrest and inhibition of cyclin A/B were achieved through the downregulation of CDK1/CDC25C in AGS cells. The current results are in agreement with our previous study, which demonstrated FKB-induced G_2/M cell-cycle arrest in human oral carcinoma HSC-3 cells and human squamous carcinoma KB cells (Hseu et al. 2012; Lin et al. 2012). Among the MAPK subfamilies, ERK pathway activation is commonly linked to the activation of cell proliferation and growth, whereas, in general, the JNK pathway contributes to cell-cycle arrest (Mingo-Sion et al. 2004). Moreover, JNK signaling has been demonstrated to be activated by intracellular ROS. To further test this hypothesis, AGS cells were pre-treated with JNK and ERK inhibitors. Our results demonstrated that a JNK inhibitor (SP600125) induced CDK1 overexpression, which was subsequently reduced when the cells were co-treated with FKB. However, this phenomenon was not identified with the ERK inhibitor (U0126) treatment. Undoubtedly, these results demonstrated that the FKB-induced G2/M phase arrest is dependent on ROS-activated JNK signaling cascades in AGS cells.

Bax is a multi-domain, pro-apoptotic, Bcl-2 family protein that plays a vital role in the intrinsic apoptotic pathway. The stimulation of various death insults leads to conformational changes in Bax, which subsequently translocates from the cytoplasm to mitochondria, thereby resulting in mitochondrial-mediated apoptosis (Marzo et al. 1998). The pro-apoptotic activity of Bax is tightly controlled by Bcl-2 protein. Bcl-2 forms heterodimers with Bax and prevents Bax oligomerization in the mitochondrial outer membrane (Oltvai et al. 1993). Thus, the Bax/Bcl-2 ratio plays a key role in the execution of intrinsic apoptosis. Our study demonstrated that the Bax protein levels were altered following FKB-induced apoptosis in NCI-N87 cells. This evidence demonstrates that a Bax conformational change is an early step in drug-induced apoptosis. Our results also demonstrated that increased Bax expression leads to mitochondria-mediated caspase activation. It is worth noting that Bax transfection reduced Bcl-2 expression and subsequently activated both caspase-3 and PARP levels in AGS cells. Furthermore, Bax-transfected cells treated with FKB, which were represented by increased TUNEL-positive cells, mirrored the increased apoptotic DNA damage. These findings strongly support the notion that Bax activation represents a highly potent apoptotic stimulus in the presence of FKB. In contrast, FKB failed to regulate the expression of autophagy in Bax-transfected AGS cells.

Beclin-1, an autophagy protein, participates in the formation of autophagosomes, which mediates the localization of other autophagy proteins to the pre-autophagosomal membrane. The interaction between Beclin-1 and Bcl-2 (anti-apoptotic protein) represents a potentially important point of convergence of the apoptotic and autophagic machinery (Pattingre et al. 2005). It has been demonstrated that Beclin-1 cannot neutralize the anti-apoptotic activity of Bcl-2; however, Bcl-2 or Bax reduces the pro-autophagic function of Beclin-1 (Kang et al. 2011). An increased Beclin-1/Bcl-2 ratio with FKB treatment indicates the induction of autophagy in gastric AGS cancer cells. This phenomenon was evidenced by the increased LC3-II accumulation and AVO formation, which contribute to the promotion of autophagic-death of gastric cancer cells. Further evidence indicates that the anti-apoptotic protein Bcl-2 acts to stabilize the mitochondrial membrane integrity via the prevention of caspase activation, Bax redistribution to the mitochondria and apoptosis (Green 2000). It has been well documented that Bcl-2 family proteins are involved in the regulation of mitochondrial-mediated apoptosis by acting as activators (Bax) or inhibitors (Bcl-2) (Thiyagarajan et al. 2015). As a result of the crucial role of Bcl-2 family proteins in the regulation of apoptosis, changes in Bcl-2 and Bax proteins and their ratios were determined in FKB-treated cells. FKB treatment downregulated pro-apoptotic Bax and the anti-apoptotic Bcl-2 expression in a similar fashion. The lack of an increase in the Bax/Blc-2 ratio with FKB further explains the unfavorable apoptotic scenario in gastric cancer cells, which did not contribute to cancer cell death.

The HER-2/PI3K/AKT/mTOR molecular signaling pathways are closely involved in the regulation of autophagy and the determination of cell fate. HER-2 is a proto-oncogene that encodes HER-2 receptor tyrosine kinase. Human gastric cancers with an overexpression of HER-2 occur in approximately 7–34% of patients and are associated with a reduced survival and a high risk of metastasis (Sukawa et al. 2014). Autophagy is a dynamic self-catabolic cellular process, which is tightly regulated by upstream modulators, most essentially the PI3K/AKT/mTOR signaling pathway (Jain et al. 2013). The PI3K-AKT pathway is one of the critical downstream signals from HER-2, and the activation of the PI3K/AKT cascade promotes mTOR activity, which is an important target

for cancer therapies (Sukawa et al. 2014). mTOR inhibits autophagy, whereas it promotes tumor cell survival, growth and proliferation (Choi 2012). In the present study, FKB treatment substantially suppressed the HER-2 activation in human gastric cancer cells. Furthermore, the suppression of HER-2 signaling by FKB is accompanied by PI3K/AKT/mTOR pathway inhibition. However, when autophagy was pharmacologically blocked by CQ, FKB-induced inhibition of the total and phosphorylated HER2, PI3K, AKT and mTOR proteins was reversed. These findings suggest that FKB-induced autophagy in AGS cells subsequently leads to the inhibition of the HER-2/ PI3K/AKT/mTOR signaling cascade.

We subsequently performed in vivo studies to further strengthen the antitumor activities of FKB using AGS-xenografted nude mice. Another important finding of this study is that FKB treatment via oral or intraperitoneal injection in xenografted nude mice (51 days) resulted in a decrease in the tumor burden during the time course, and this antitumor activity was more prominent compared with the oral administration. The decreased tumor volume and weight with FKB is linked with a remarkable decrease in mitotic cells in the tumor sections. Decreased mitotic cells in tumors implies a decreased proliferating ability of cancer cells that may result in a decrease in the tumor volume. In accordance with in vitro autophagic-cell death, FKB treatment in mice also induced autophagy in tumors as evidenced by increased LC3-II accumulation and Beclin-1 and ATG7 expressions. Despite the in vivo findings, the in vitro results indicated there was no change in Beclin-1 in the AGS cells following FKB treatment. In addition, the decreased tumor burden contributed to a prolonged survival rate in nude mice following long-term FKB treatment. Taken together, our in vivo data confirm that FKB treatment controlled tumor development via the induction of autophagic pathways.

Recently, an interest in autophagy has been renewed among tumor biologists because different types of cancer cells undergo autophagy after various anticancer therapies. Studies have demonstrated that similar to apoptosis, autophagy is important in the regulation of cancer progression and development in determining the response of tumor cells to anticancer therapy (Thiyagarajan et al. 2016). The autophagy pathway is controlled by evolutionarily conserved autophagy-related ATG proteins, which are involved in enucleation and elongation during autophagosome formation (Klionsky and Emr 2000). LC3, a mammalian homolog of yeast ATG8, is a highly sensitive molecular marker of autophagosomes. LC3 undergoes post-translational modification during autophagy, and it is cleaved at the carboxy terminus to form soluble LC3-I. LC3-I is subsequently modified to a membrane-bound form, referred to as LC3-II, which is recruited onto autophagosomes (Mohan et al. 2013). Therefore, the ratio of the LC3-I and LC3-II levels was used as a specific marker to reflect the activation of autophagy. In the present study, silencing of LC3 expression by shRNA was demonstrated to abrogate the FKB-induced decreased cell viability and colony formation ability of AGS cells. The observed cancer cell death was associated with the FKB-induced activation of autophagy-associated signaling in AGS cells. Furthermore, the in vivo data indicated that FKB-induced inhibition of tumor growth was attenuated by shLC3. These pre-clinical findings confirmed that autophagy is the main cell death mechanism, which is mediated by FKB, in human gastric cancer cells.

In conclusion, the present study sheds new light on the detailed molecular mechanisms involved in FKB-triggered autophagy. Our results indicate that FKB-induced cell death is mediated by ROS-induced caspase-independent autophagy both in vitro and in vivo. Taken together, our findings suggest that FKB may be an effective chemotherapeutic agent against human gastric cancer.

Acknowledgements This work was supported by Grants MOST-104-2320-B-039-040-MY3, MOST-103-2320-B-039-038 -MY3, NSC-103-2622-B-039-001-CC2, CMU103-ASIA-12, and CMU 103-ASIA-09 from the Ministry of Science and Technology, Asia University, and China Medical University, Taiwan to Dr. Hsin-Ling Yang and Dr. You-Cheng Hseu. This study was supported by China Medical University under the Aim for Top University Plan of the Ministry of Education, Taiwan (CHM106-5-3).

Compliance with ethical standards

Conflict of interest The authors declare that there is no conflict of interest.

References

Abu N, Ho WY, Yeap SK, Akhtar MN, Abdullah MP, Omar AR, Alitheen NB (2013) The flavokawains: uprising medicinal chalcones. Cancer cell Int 13:102 doi:10.1186/1475-2867-13-102

Abu N et al (2015) In vivo antitumor and antimetastatic effects of flavokawain B in 4T1 breast cancer cell-challenged mice. Drug Des Devel Ther 9:1401–1417 doi:10.2147/DDDT.S67976

Carreñ OI LE, Martelloni A, Salas B, Simõ es BG, Vergona PR (2014) German court repeals the withdrawal of marketing authorisation of kava-containing medicinal products Trade. Perspectives 13:2–5

Choi KS (2012) Autophagy and cancer. Exp Mol Med 44:109–120 doi:10.3858/emm.2012.44.2.033

Clayton NP, Yoshizawa K, Kissling GE, Burka LT, Chan PC, Nyska A (2007) Immunohistochemical analysis of expressions of hepatic cytochrome P450 in F344 rats following oral treatment with kava extract. Exp Toxicol Pathol 58:223–236 doi:10.1016/j.etp.2006.08.002

DiSilvestro RA, Zhang W, DiSilvestro DJ (2007) Kava feeding in rats does not cause liver injury nor enhance galactosamine-induced hepatitis. Food Chem Toxicol 45:1293–1300. doi:10.1016/j.fct.2007.01.015

Green DR (2000) Apoptotic pathways: paper wraps stone blunts scissors. Cell 102:1–4. doi:10.1016/S0092-8674(00)00003-9

Hale AN, Ledbetter DJ, Gawriluk TR, Rucker EB 3rd (2013) Autophagy: regulation and role in development. Autophagy 9:951–972. doi:10.4161/auto.24273

Hasima N, Ozpolat B (2014) Regulation of autophagy by polyphenolic compounds as a potential therapeutic strategy for cancer. Cell Death Dis 5:e1509 doi:10.1038/cddis.2014.467

Hseu YC et al (2012) The chalcone flavokawain B induces G2/M cell-cycle arrest and apoptosis in human oral carcinoma HSC-3 cells through the intracellular ROS generation and downregulation of the Akt/p38 MAPK signaling pathway. J Agric Food Chem 60:2385–2397. doi:10.1021/jf205053r

Hsin IL et al (2010) *N*-acetyl cysteine mitigates curcumin-mediated telomerase inhibition through rescuing of Sp1 reduction in A549 cells. Mutat Res. doi:10.1016/j.mrfmmm.2010.03.011

Huang CC, Lien HH, Sung YC, Liu HT, Chie WC (2007) Quality of life of patients with gastric cancer in Taiwan: validation and clinical application of the Taiwan Chinese version of the EORTC QLQ-C30 and EORTC QLQ-STO22. Psychooncology 16:945–949. doi:10.1002/pon.1158

Jain K, Paranandi KS, Sridharan S, Basu A (2013) Autophagy in breast cancer and its implications for therapy. A J Cancer Res 3:251–265

Kang R, Zeh H, Lotze M, Tang D (2011) The Beclin 1 network regulates autophagy and apoptosis. Cell Death Differ 18:571–580

Karna P, Zughaier S, Pannu V, Simmons R, Narayan S, Aneja R (2010) Induction of reactive oxygen species-mediated autophagy by a novel microtubule-modulating agent. J Biol Chem 285:18737–18748. doi:10.1074/jbc.M109.091694

Klionsky DJ, Emr SD (2000) Autophagy as a regulated pathway of cellular degradation. Science 290:1717–1721

Komoto M et al (2009) HER2 overexpression correlates with survival after curative resection of pancreatic cancer. Cancer Sci 100:1243–1247. doi:10.1111/j.1349-7006.2009.01176.x

Kondo Y, Kanzawa T, Sawaya R, Kondo S (2005) The role of autophagy in cancer development and response to therapy. Nat Rev Cancer 5:726–734. doi:10.1038/nrc1692

Lin E et al. (2012) Flavokawain B inhibits growth of human squamous carcinoma cells: involvement of apoptosis and cell cycle dysregulation in vitro and in vivo. J Nutr Biochem 23:368–378 doi:10.1016/j.jnutbio.2011.01.002

Marzo I et al (1998) Bax and adenine nucleotide translocator cooperate in the mitochondrial control of apoptosis. Science 281:2027–2031

Mingo-Sion AM, Marietta PM, Koller E, Wolf DM, Van Den Berg CL (2004) Inhibition of JNK reduces G2/M transit independent of p53, leading to endoreduplication, decreased proliferation, and apoptosis in breast cancer cells. Oncogene 23:596–604. doi:10.1038/sj.onc.1207147

Mohan N, Chakrabarti M, Banik NL, Ray SK (2013) Combination of LC3 shRNA plasmid transfection and genistein treatment inhibited autophagy and increased apoptosis in malignant neuroblastoma in cell culture and animal models. PLoS One 8:e78958. doi:10.1371/journal.pone.0078958

Munshi A, Ramesh R (2013) Mitogen-activated protein kinases and their role in radiation response. Genes Cancer 4:401–408 doi:10.1177/1947601913485414

Narayanapillai SC, Leitzman P, O'Sullivan MG, Xing C (2014) Flavokawains a and B in kava, not dihydromethysticin, potentiate acetaminophen-induced hepatotoxicity in C57BL/6 mice. Chem Res Toxicol 27:1871–1876 doi:10.1021/tx5003194

Nowakowska Z (2007) A review of anti-infective and anti-inflammatory chalcones. Eur J Med Chem 42:125–137 doi:10.1016/j.ejmech.2006.09.019

Ohsumi Y (2001) Molecular dissection of autophagy: two ubiquitin-like systems. Nat Rev Mol Cell Biol 2:211–216. doi:10.1038/35056522

Oltvai ZN, Milliman CL, Korsmeyer SJ (1993) Bcl-2 heterodimerizes in vivo with a conserved homolog, Bax, that accelerates programmed cell death. Cell 74:609–619

Ozpolat B, Dalby K, Berestein GL (2012) Induction of autophagy by polyphenolic compounds in cancer: a novel Strategy to induce cell death and to treat Cancer. In: Diederich M, Noworyta K (eds) Natural compounds as inducers of cell death, vol 1. Springer, Dordrecht, pp 237–261

Pan MH, Ho CT (2008) Chemopreventive effects of natural dietary compounds on cancer development. Chem Soc Rev 37:2558–2574 doi:10.1039/b801558a

Pattingre S et al (2005) Bcl-2 antiapoptotic proteins inhibit Beclin 1-dependent autophagy. Cell 122:927–939. doi:10.1016/j.cell.2005.07.002

Pelicano H, Carney D, Huang P (2004) ROS stress in cancer cells and therapeutic implications. Drug Resist Updat 7:97–110 doi:10.1016/j.drup.2004.01.004

Qiao S et al (2015) A REDD1/TXNIP pro-oxidant complex regulates ATG4B activity to control stress-induced autophagy and sustain exercise capacity. Nat Commun 6:7014. doi:10.1038/ncomms8014

Rothe K et al (2014) The core autophagy protein ATG4B is a potential biomarker and therapeutic target in CML stem/progenitor cells. Blood 123:3622–3634. doi:10.1182/blood-2013-07-516807

Singh YN, Devkota AK (2003) Aqueous kava extracts do not affect liver function tests in rats. Planta Med 69:496–499 doi:10.1055/s-2003-40658

Sorrentino L, Capasso A, Schmidt M (2006) Safety of ethanolic kava extract: results of a study of chronic toxicity in rats. Phytomedicine 13:542–549 doi:10.1016/j.phymed.2006.01.006

Steiner GG (2000) The correlation between cancer incidence and kava consumption. Hawaii Med J 59:420–422

Sukawa Y et al (2014) HER2 expression and PI3K-Akt pathway alterations in gastric cancer. Digestion 89:12–17. doi:10.1159/000356201

Tanida I, Ueno T, Kominami E (2004) LC3 conjugation system in mammalian autophagy. Int J Biochem Cell Biol 36:2503–2518 doi:10.1016/j.biocel.2004.05.009

Teschke R (2010) Kava hepatotoxicity–a clinical review. Ann Hepatol 9:251–265

Thiyagarajan V, Tsai MJ, Weng CF (2015) Antroquinonol targets FAK-signaling pathway suppressed cell migration, invasion, and tumor growth of C6 glioma. PLoS One 10:e0141285. doi:10.1371/journal.pone.0141285.PONE-D-15-20248

Thiyagarajan V, Sivalingam KS, Viswanadha VP, Weng CF (2016) 16-hydroxy-cleroda-3,13-dien-16,15-olide induced glioma cell autophagy via ROS generation and activation of p38 MAPK and ERK-1/2. Environ Toxicol Pharmacol 45:202–211 doi:10.1016/j.etap.2016.06.005

Wagner EF, Nebreda AR (2009) Signal integration by JNK and p38 MAPK pathways in cancer development. Nat Rev Cancer 9:537–549. doi:10.1038/nrc2694

Xie CM, Chan WY, Yu S, Zhao J, Cheng CH (2011) Bufalin induces autophagy-mediated cell death in human colon cancer cells through reactive oxygen species generation and JNK activation. Free Radic Biol Med 51:1365–1375. doi:10.1016/j.freeradbiomed.2011.06.016

Zhang X, Chen LX, Ouyang L, Cheng Y, Liu B (2012) Plant natural compounds: targeting pathways of autophagy as anti-cancer therapeutic agents. Cell Prolif 45:466–476 doi:10.1111/j.1365-2184.2012.00833.x

Zhang Z et al (2013) Wentilactone B induces G2/M phase arrest and apoptosis via the Ras/Raf/MAPK signaling pathway in

human hepatoma SMMC-7721 cells. Cell Death Dis 4:e657 doi:10.1038/cddis.2013.182

Zhang H et al (2014) Harmine induces apoptosis and inhibits tumor cell proliferation, migration and invasion through down-regulation of cyclooxygenase-2 expression in gastric cancer. Phytomedicine 21:348–355 doi:10.1016/j.phymed.2013.09.007

Zhao Y, Wu Z, Zhang Y, Zhu L (2013) HY-1 induces G(2)/M cell cycle arrest in human colon cancer cells through the ATR-Chk1-Cdc25C and Weel pathways. Cancer Sci 104:1062–1066. doi:10.1111/cas.12182

Zhou P et al (2010) Flavokawain B, the hepatotoxic constituent from kava root, induces GSH-sensitive oxidative stress through modulation of IKK/NF-kappaB and MAPK signaling pathways. FASEB J 24:4722–4732. doi:10.1096/fj.10-163311

Zhou H et al (2014) Ciclopirox induces autophagy through reactive oxygen species-mediated activation of JNK signaling pathway. Oncotarget 5:10140–10150. doi:10.18632/oncotarget.2471

Zi X, Simoneau AR (2005) Flavokawain A, a novel chalcone from kava extract, induces apoptosis in bladder cancer cells by involvement of Bax protein-dependent and mitochondria-dependent apoptotic pathway and suppresses tumor growth in mice. Cancer Res 65:3479–3486. doi:10.1158/0008-5472.CAN-04-3803